AN ABSTRACT OF THE THESIS OF

Thidarat Dendamrongvit for the degree of Master of Science in Industrial Engineering presented on May 1, 2002.
Title: Development of a Posture Prediction Model.

Redacted for Privacy

Abstract approved: _____
Jeffrey C. Woldstad

Biomechanical models have been used in designing human work environments to evaluate potential risks to workers before a work environment is constructed. In order for work environments to be modeled correctly, most biomechanical models require as input, an accurate body posture of the worker. This information can be obtained by, either measuring the posture of workers for the task of interest, or estimating the posture.

This research explores methods to estimate working postures by developing a model that can predict a worker's posture. The model in this thesis represents the body of the worker with ten links: neck, left and right forearms, left and right upper arms, body, left and right thighs, and left and right calves. The work task inputs consist of the magnitude and direction of the force applied to the hands, and the distances between the hands and the floor. By using these inputs, the model can predict a posture by optimizing an objective function of two criteria: Total Squared

Moment and Balance. Model constraints also ensure that a predicted posture is feasible for human.

The output of the model is the predicted posture in terms of ten body joint angles: neck, left and right elbows, left and right shoulders, hip, left and right knees, left and right ankles. These joint angles are defined as angles relative to horizontal.

The prediction posture can be used as a base reference when inputting into other biomechanical models. By predicting posture from the model, one can obtain postures of the workers without direct measurement of postures from the workers, which can be expensive and time consuming.

Development of a Posture Prediction Model

by
Thidarat Dendamrongvit

A THESIS

submitted to

Oregon State University

in partial fulfillment of
the requirements for the
degree of

Master of Science

Presented May 1, 2002
Commencement June 2002

Master of Science thesis of Thidarat Dendamrongvit presented on May 1, 2002.

APPROVED:

Redacted for Privacy

Major Professor, representing Industrial Engineering

Redacted for Privacy

Head of the Department of Industrial and Manufacturing Engineering

Redacted for Privacy

Dean of the Graduate School

I understand that my thesis will become part of the permanent collection of Oregon State University libraries. My signature below authorizes release of my thesis to any reader upon request.

Redacted for Privacy

Thidarat Dendamrongvit, Author

ACKNOWLEDGEMENTS

I would like to thank Dr. Jeffrey Woldstad for his understanding and support throughout my thesis work and Dr. David Kim for his help and suggestions. I also want to thank Dr. Kimberly Douglas for her support in many ways while I have been studying here. I would like to express my appreciation to Dr Solomon Yim for serving as my committee member.

In addition, thanks are due to the Department of Industrial and Manufacturing Engineering for making my study life here at Oregon State University invaluable.

A very special thanks to my family, I am grateful for their love, encouragement, support, and everything.

TABLE OF CONTENTS

TABLE OF CONTENTS (Continued)

TABLE OF CONTENTS (Continued)

LIST OF FIGURES

LIST OF FIGURES (Continued)

LIST OF TABLES

LIST OF APPENDIX FIGURES

Development of a Posture Prediction Model

1. INTRODUCTION

1.1. Rationale

Ergonomics plays an important role in designing the human work environment. It impacts people and reduces the hazards present in the workplace. Computer-aided design (CAD) tools have been used by ergonomists as a method to analyze work tasks and work environments. These methods are being used in the equipment design process to evaluate potential risks to workers before a work environment is constructed. The computer tools can be used to predict quantities such as reach lengths, forces, strength capabilities, and motion paths. However, for work environments to be modeled correctly, most computer tools require as input, an accurate body posture of the worker. This information can be obtained by either measuring the posture of workers for the task of interest, or estimating the posture.

This research investigates methods to estimate working postures by using a posture prediction model. Measurement methods such as direct observation can be expensive, difficult, and time-consuming. Therefore, it is important to find accurate methods to estimate working postures in the absence of measurement. Accurate posture prediction models can reduce the time and effort involved in using computer tools by reducing the need to measure and record body posture.

1.2. Thesis Description

The model in this thesis represents the body of the worker with ten links: neck, left and right forearm, left and right upper arm, body, left and right thigh, left and right calf. The model also requires as two types of inputs; those associated with the worker, and those associated with the work task. Inputs associated with the human worker consist of the link lengths, the link weights, the link center-of-mass locations, and the weight of the whole body. The work task inputs consist of the magnitude and direction of the force applied to the hands, and the distances between the hands and the floor.

Using these inputs, the model then predicts posture by optimizing multiple biomechanical and behavioral criteria. The output of the model is the predicted posture in terms of ten body joint angles (the decision variables in the optimization model): neck, left and right elbows, left and right shoulders, hip, left and right knees, left and right ankles.

Model constraints ensure that feasible postures are identified by the model. These constraints require that all joint angles stay within a defined range of motion specified by a minimum angle and a maximum angle. Additional constraints enforce a stable or balanced posture, and a visible hand position. Nonlinear optimization is used to find the optimal posture based on a convex combination of two criteria. The first criterion is the effort required to maintain a specific posture, where effort is defined as the sum of the squared moments about each joint

(Woldstad, 1994). The second criterion is balance, expressed as the sum of the squared moments about the balls and heels of the feet. Minimizing the first criteria was shown to be effective for predicting static plane body postures with some degree of accuracy (Woldstad, 1994). Minimizing the second criteria attempts to obtain the "most balanced" posture.

A model that can predict a human posture associated with work tasks was developed. The model will be based on the following criteria and constraints.

Model criteria: Minimize the sum of the squared moments about each joint and the sum of the squared moments about the balls and heels of the feet.

Model constraints: range of motion, balance, and visible hand position.

1.3. Thesis Objectives

The objectives of this thesis were:

Objective 1: Develop a model that can predict a posture for the worker by representing two sides of the human body (i.e., with two arms and two legs).

Objective 2: Develop a posture prediction model using multi-objective optimization including both moment and balance criteria in the objective function.

Objective 3: Demonstrate that the model can predict the postures.

1.4. Thesis Organization

This thesis is divided into 5 chapters. The following chapter is the Literature Review describing prior research in the area of biomechanical and posture prediction models. The Model Development chapter will describe the details of the posture prediction model. The model results using different load directions with three different hand positions will be shown in Simulation Results, followed by Discussions.

2. LITERATURE REVIEW

This literature review is divided into three sections. First, a description of biomechanical models, motivation for their development, and example applications are presented. Research in the field of biomechanical modeling using an optimization approach is discussed in the second section. Literature investigating posture and motion prediction modeling are discussed in the third section. Finally, a summary of the literature review is provided in the fourth section.

2.1. Biomechanical Models

Biomechanical models are mathematical representations of the musculoskeletal system that are developed to understand or interpret the functional behavior and joint loadings that occur during a task or exertion of interest (Granata and Marras, 1996). Biomechanical models calculate physical stresses associated with the effects of internal and external forces in various body joints during movement. These stresses can then be compared with accepted limits.

Granata and Marras (1996) explained that the goal of biomechanical modeling in an ergonomics context is to gain insight into how the joints of the body are strained during work as well as to provide a framework for understanding how the musculoskeletal system behaves during work task performance. They also

stated that biomechanical models provide qualitative and quantitative answers that explain how the body is loaded during work as follows.

1. Qualitative analyses allow comparison of biomedical loads between two or more sets of conditions. For example, models of musculoskeletal stresses may allow ergonomists to determine which of several workstation designs will result in the least amount of structural loading on a specific joint.
2. Quantitative analyses allow one to address the issue of how much is too much loading on a joint. Quantification can both assess the risk associated with existing jobs and predict whether a proposed workstation can be expected to lead to injuries for humans.

Chaffin (1999) described three reasons to develop biomechanical models. First, the models are a representation of the real system. Model's behavior and actual behavior of the system can be compared in order to obtain the outcomes. The models help gain insight into the complicated actual system. Second, biomechanical models provide information of real situations. Due to time and cost constraints, it may not be possible to set up a laboratory representation of a task. Biomechanical models can help to interpolate and extrapolate limited musculoskeletal capacity data from different sources. Finally, a biomechanical model is the only way to predict potentially hazardous loading conditions on certain musculoskeletal components in some work situations.

Biomechanical models have been developed for many different applications including: a model for the design of manual work stations (Kilpatrick, 1970), a geometric model of the human torso (Nussbaum and Chaffin, 1995), a model for the simulation of torso muscle coordination (Nussbaum et al., 1997), models of the hand (Chao et al., 1976; Landsmeer, 1963), models of the wrist (Armstrong and Chaffin, 1978; Marras et al., 1993), a model of the arm (Hughes et al., 1997), models of the trunk (Brinckmann et al., 1988; Shirazi-Adl, 1989; Marras et al., 1984;), and a model of the back (Marras et al., 1995).

Most biomechanical models require the posture of the worker as an input. The posture of the worker can be either measured or predicted. However, measurement of the posture can be expensive and time consuming. The biomechanical model developed in this thesis is a posture prediction model which can predict a posture instead of measuring it. By using a posture prediction model, a posture can be predicted with less cost than the measurement method.

The goal of many whole body posture prediction models is to predict the angles of each link knowing the hand position relative to a base such as the ankle or the intervertebral joint L5/S1 (Dysart, 1994). The model in this thesis is a ten-link whole body lifting static model where links represent bone links and the end points of the link represent the joints of the body. The orientation of the links is defined by angles.

2.2. Optimization in Biomechanical Models

Optimization involves finding the best solution to a problem (Beale, 1988). When the problem consists of an objective function and a set of constraint equations, it can have an indeterminate solution because there may be not enough equations so that the exact values of the variables in the objective function and constraints can be found. In that case, optimization is an effective way to find the answer. In biomechanical models, it is assumed that humans are likely to choose to perform tasks where they feel optimum in terms of biomechanical criteria such as minimum joint compression, maximum joint strength, or minimum fatigue. Optimization-based models have been used to find the optimal solution to many problems in biomechanics. The following biomechanical models employ an optimization approach in different applications involving human movement.

Hirao and Yamazaki (1997) developed a simulation model of the body and chair system in order to improve conventional trial-and-error manufactures in chair design. The model predicts the natural sitting posture corresponding to a chair condition. They considered the loads on the musculoskeletal system and soft tissues for evaluation of sitting posture. They constructed two models in the sagittal plane: a musculoskeletal model composed of 13 rigid links representing body segments and a finite element model representing soft tissues of body surface. The soft tissues of the body surface were classified with parts of muscle and fat. Chair parameters were cushion properties such as elastic elements, dimensions,

angles and surface shapes. They calculated mechanical equilibriums between these models simultaneously and synthesized the sitting posture. The sitting postures were predicted based on biomechanical criteria and conditions. The models employed criteria for minimizing back muscle stress, neck muscle stress, shear forces of intervertebral discs, and reaction forces acting on the thigh. A nonlinear optimization method (as shown in Figure 2.1) was developed for predicting sitting postures by mechanical equilibrium between the musculoskeletal model and the finite element model. The Semi-Newton method was employed for optimization.

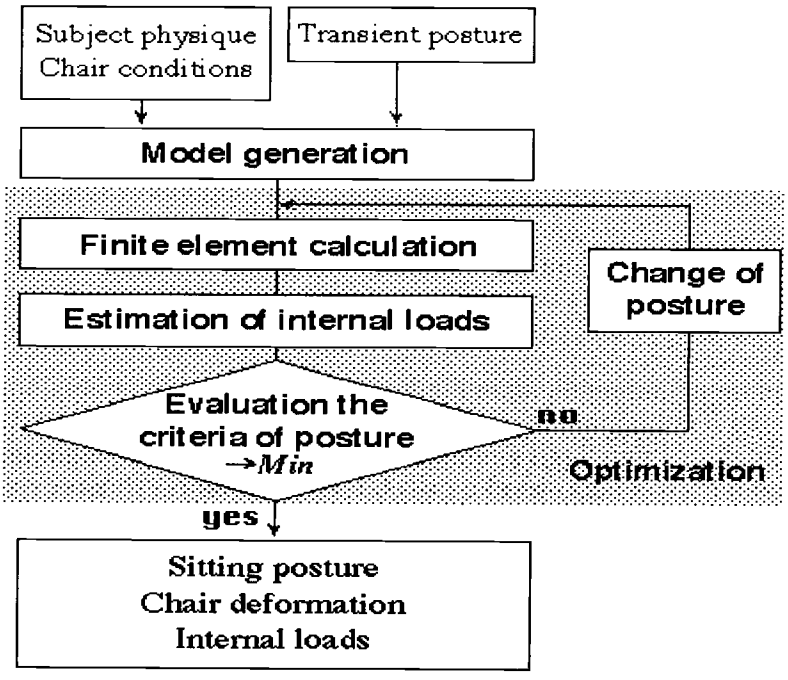

Figure 2.1: Calculation flow of the simulation model of body and chair system (adapted from Hirao and Yamazaki, 1997).

Bean et al., (1988) proposed the Minimum Intensity Compression (MIC) model describing low-back musculoskeletal system biomechanics. The model used double objective linear programming to calculate muscle contraction forces. The problem had an indeterminate solution because there were at most six equations of equilibrium (three force equations and three moment equations) to be satisfied, but there were often more than six muscle forces to be calculated. They proposed an alternative which involves formulating and solving two linear programs sequentially. The first linear program minimized maximum muscle intensity. The second linear program minimized the sum of the muscle forces using the solution from the first model as the intensity limit. Each linear programming had three sets of constraints with unknown muscle forces. The first set of constraints used moment equilibrium equations. The second set of constraints required that the intensity of each muscle contraction be not greater than the maximum intensity while intensity was determined as the force exerted by the muscle divided by its cross-sectional area. The last set required that all muscle forces be non-negative since muscles do not sustain compression forces. The first model including the objective function and set of constraint equations is shown in the following page.

$$\text{Min } I \tag{2.1}$$

$$\text{subject to: } \sum_{j=1}^{m} a_{ij}x_j = b_i, \quad i = 1, 2, 3 \tag{2.2}$$

$$d_j x_i \leq I, \quad j = 1, 2, \ldots, m \tag{2.3}$$

$$x_j \geq 0, \quad j = 1, 2, \ldots, m \tag{2.4}$$

where,

m is the number of muscles modeled.

a_{ij} is the component of the moment arm of muscle j about axis i.

b_i is the component of the external moment about axis i.

d_i is the inverse of the cross-sectional area of muscle j.

These are the known parameters of the model. The following parameters are unknown.

x_j is the muscle forces for muscle j.

I is the resultant maximum intensity.

The second model including objective function and set of constraint equations is shown below.

$$\min \sum_{j=1}^{m} x_j \tag{2.5}$$

$$\text{subject to: } \sum_{j=1}^{m} a_{ij}x_j = b_i, \quad i = 1, 2, 3 \tag{2.6}$$

$$d_j x_i \leq I, \quad j = 1, 2, \ldots, m \tag{2.7}$$

$$x_j \geq 0, \quad j = 1, 2, \ldots, m \tag{2.8}$$

where I is now considered fixed and only the x_j are the unknowns.

A unique optimal solution can be found from this approach. Because of low computation cost and stability of solutions, the double linear programming approach could also be used to calculate solution sensitivity to investigate the effects of errors in posture measurement and errors in the orthogonal cutting plane selected.

McMulkin (1996) investigated the ability of optimization-based biomechanical models to predict torso muscular activity for a lifting task. He considered two optimization models: the Minimum Intensity Compression (MIC) on Bean et al., (1988) described above, and the Sum of the Cubed Intensities (SCI) model. The SCI model has an objective function to minimize the sum of the cubed muscle intensities subject to the moment equilibrium constraints. The SCI model was formulated as follows:

$$\text{Min} \quad \sum_{i=1}^{m} (f_i/A_i)^3 \tag{2.9}$$

$$\text{Subject to} \quad \sum_{i=1}^{m} |f_i| (r_i \times \tau_i) + \mathrm{M}^E \tag{2.10}$$

$$f_i \geq 0 \tag{2.11}$$

$$A_i \geq 0 \tag{2.12}$$

where,

m is the number of muscles.

f_i is the tension in each muscle.

A_i is the cross-sectional area of each muscle.

r_i is the moment arm vector.

τ_i is the muscle line of action.

M^E are the externally applied moments in three-dimensions.

These models use the concepts of mathematical programming to estimate the muscle forces in the human body. He used regression techniques to assess the accuracy of model predictions. He found that the SCI model had a better correlation between the predicted and actual muscle activity across subjects. Therefore, overall the SCI model provided better predictions than the MIC model.

Kerk (1992) developed a two-dimensional optimization biomechanical model to predict maximum static hand force exertion capability. This mathematical biomechanical model combines 3 constraints in predicting hand force: strength, stability, and coefficient of friction (COF). He expressed these constraints in a linear form. Thus, the model can calculate an optimal hand force solution for a specific objective function. He proposed a set of 11 specific objective functions: maximize pure push force, maximize pure pull force, maximize pure lift force, maximize pure press down force, maximize net push force, maximize net pull force, maximize net lift force, maximize net press down force, maximize hand force (regardless of direction), minimize hand force (regardless of direction), and maximize hand force with respect to a specific direction.

He conducted experiments by using eight subjects to isolate and evaluate the effects of strength, stability, and the coefficient of friction on hand force

exertion capability. The model was used to simulated posture/force exertion combinations that would demonstrate the existence and importance of each individual constraint. In the case of the strength constraints, the results showed important differences in the observed force exertion angle versus the optimal angle predicted by the model. The portions of the experiment which evaluated the stability and coefficient of friction constraints had the results that hand force exertion capability could be constrained by factors other than strength capability. He concluded that hand force exertion capability should be considered identically by stability and coefficient of friction along with strength capability.

Kerk (1992) also developed a three-dimensional model which expanded his two-dimensional model. His three-dimensional model included the torso and asymmetric upper and lower extremities to predict maximum static force exertion with constraints of stability, strength, and the coefficient of friction. The model had a comprehensive ability to combine multiple factors that can affect hand force exertion capability under asymmetric, three-dimensional conditions. Although experiment evaluation of the three-dimensional model would be future work in his research, his three-dimensional hand force exertion capability model offered important improvements over the two-dimensional one because the graphical depiction of the three-dimensional model described important physical interpretations.

2.3. Posture and Motion Prediction Models

Posture is a composite of the positions of all the joints of the body at any given moment. Posture prediction models have been developed to represent how people of a particular anthropometry choose a working posture under defined conditions.

There have been two different approaches to creating posture prediction models (Dysart, 1994): regression models and inverse kinematic models. Each of these is briefly described in the following sections.

1. Regression models

This traditional method uses anthropometrical data collecting from several experiments by human subjects, or simulation using three-dimensional computer-aided man modeling software, to form a predictive model of posture by using regression models (Abdel-Malek et al., 2001). The dependent variables are expressed as a linear or nonlinear combination of a function of independent variables. The model assumptions of regression models are described below (Ramsey and Schafer, 1997).

- There is a normally distributed subpopulation of dependent variables for each value of the independent variable.
- The subpopulation standard deviations are all equal.
- The selection of an observation from any of the subpopulations is independent of the selection of any other observation.

Some of the regression models to predict posture have been proposed by Kilpatric (1970), who developed regression equations to predict the posture of the upper body (elbow, shoulder, and back), Anderson et al., (1986), who developed a nonlinear second order regression equation to predict equations for sacral/pelvic rotation about the hip joint and L5 rotation, and Faraway (2001), who modeled variability within the reaches of a given subject and that between subjects in reaching motions by using regression equations.

2. Inverse kinematics

Inverse kinematics is concerned with the determination of joint variables of a manipulator given its final position. Models using the inverse kinematics method have a known end point, and the problem is to calculate the angles. The solution is indeterminate in many cases because it can come up with many different solutions. Therefore, a specific criterion is used in order to end up with an optimal solution. There has been work using inverse kinematics solutions in the robotics field. This thesis uses the inverse kinematics method to develop a posture prediction model. The end points (hand positions) are known. The orientation which is defined by angles is determined based on criteria and conditions.

Inverse kinematics models to predict posture have been proposed by Byun (1991), who developed a 2-D posture prediction algorithm that predicts isometric postures knowing the hand locations relative to the ankle, and Jung et al., (1992),

who predicted the 3-D path of the upper limb (wrist, elbow, and shoulder) performing a reaching task.

The literature shows that there have been models developed to predict posture and motion. Posture prediction models involve predicting posture in a static position. Posture prediction models are representations of static postures doing tasks of interest such as lifting. On the other hand, motion simulations can be represented as series of static postures linked together in time to give the illusion of motion pictures (Granata et al., 1996). The following are some examples of both types of prediction models.

2.3.1. Posture Prediction Models

Anderson et al., (1986) developed a model that predicts sacral/pelvic rotation about the hip joint and L5 rotation relative to the sacrum for lifting tasks in the sagittal plane. They had two males and two females isometrically pull in a vertical direction on a set of handles in 22 postures at various knee and torso angles ranging from erect standing to a deep squat. The subjects attempted lifts at three force levels at each posture. Joint angles were recorded photographically. Eight body angles were calculated (knee angle, thigh angle, torso angle, pelvic angle, sacral angle, L5 angle, L3 angle, T12 angle). The model consisted of regression equations that were developed to predict the rotation angle of the sacrum and relative L5/sacrum rotation. In the regression model, rotation angle was the

dependent variable while torso angle, knee angle, and percent of maximum load in hands were included as independent variables. The rotation pattern as functions of posture had been found. The most of the rotation occurred in the lumbar region at the beginning of flexion, but slowly shifts to rotation of the sacrum about the hip joint, starting at about 50 degrees torso rotation. After that, sacral rotation predominates and the relative L5/S1 orientation remained fixed. They also found that as knee angle decreased, the relative amount of sacral rotation decreased and L5/S1 rotation increased. It can be concluded that the degree of sacral rotation about the hip joint and L5 rotation relative to the sacrum in static postures is influenced primarily by torso angle and knee angle.

Lim et al., (1999) claimed that the model developed by Anderson et al., (1986) would not be appropriate to predict a reach posture, since a reach is a composite motion of trunk flexion and trunk lateral bending. Lim et al., (1999) developed another reach posture prediction model with a two-segment trunk model by considering the lean direction. The lean direction is defined from the hip joint, as shown in Figure 2.2.

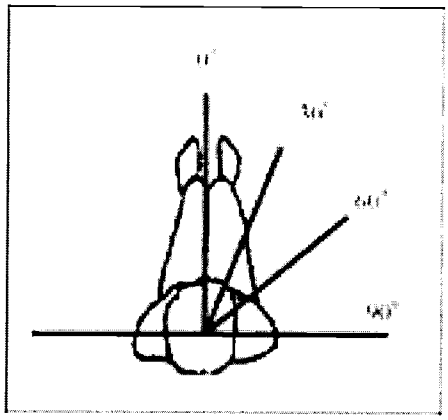

Figure 2.2: Lean direction of trunk motion (adapted from Lim et al., 1999).

The trunk was divided into two links: pelvis link, referring to the link from the hip joint to L5/S1, and lumbar-thoracic link, which is the link from L5/S1 to sternum as shown in Figure 2.3.

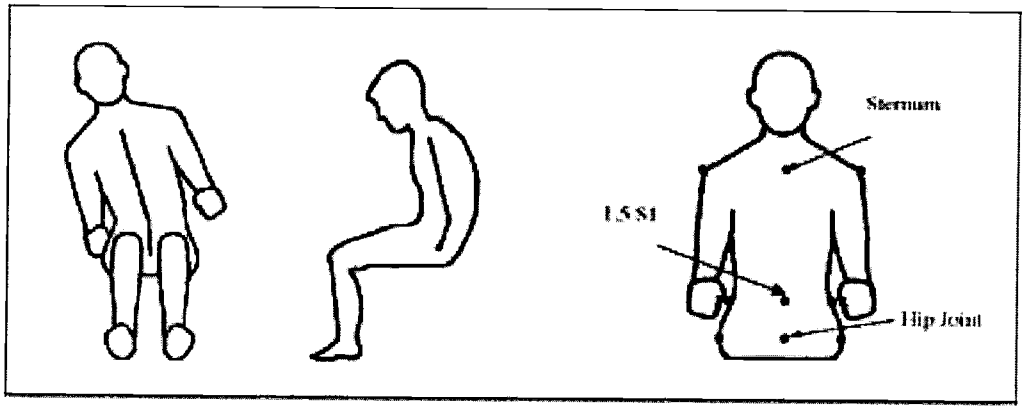

Figure 2.3: A two-segment trunk model (adapted from Lim et al., 1999).

During a reach, the motions of the trunk, pelvis link, and lumbar-thoracic link were represented as a triangle, as shown in Figure 2.4.

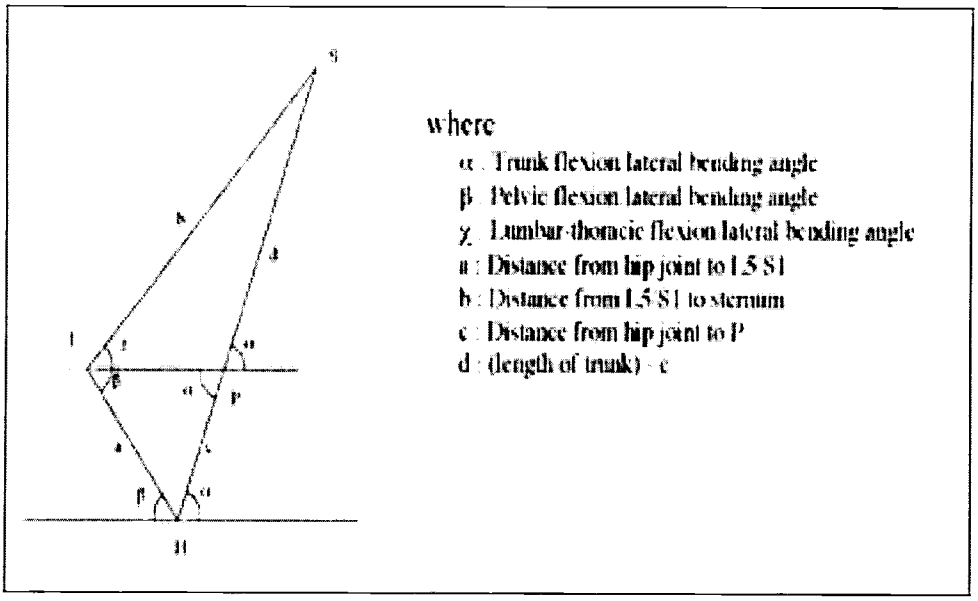

Figure 2.4: Relationships between the trunk, pelvis link and lumbar-thoracic link (adapted from Lim et al., 1999).

The lumbar-thoracic flexion/lateral bending against the trunk flexion/lateral bending were expressed as:

$$c = a\frac{\sin\beta}{\sin\alpha} \tag{2.13}$$

$$\chi = \sin^{-1}(\frac{d}{b}\sin\alpha) \tag{2.14}$$

They had six male subjects perform in two experiments: measurement of pelvis angles against trunk angles, and measurement of reach motion. In the experiments, the subjects were seated with comfortable postures. In the first experiment, the subjects flexed the trunk, following the lean direction, as much as possible without any separation of the buttocks from the seat. In the second experiment, the subjects had a marker attached to their hands, wrists, elbows, right and left shoulders, right and left hip joints. Then, they reached eight target positions with different dimensions. Regression equations for two-segment trunk motion were obtained. Pelvic flexion angle, lumbar-thoracic flexion angle, pelvic lateral bending angle, and lumbar-thoracic lateral bending angle were dependent variables while trunk flexion angle and trunk lateral bending angle were independent variables. The results showed a linear relationship between pelvic flexion angles and trunk flexion angles, and a quadratic relationship between the pelvic lateral bending angle and the trunk lateral bending angle. They also found that lean direction did not effect systematically on the two-segment trunk motion.

Jung, Kee, and Chung (1995) developed a model to predict upper body reach posture. This model is intended to be used for ergonomic workspace design and computer-aided ergonomic evaluation models or CAD systems. They used an analytic reach prediction algorithm by employing the inverse kinematics method. The model presents the upper limb as a four-link system, consisting of trunk, upper

arm, lower arm, and hand with a total of eight degrees of freedom. The link system of the right upper limb is shown in Figure 2.5.

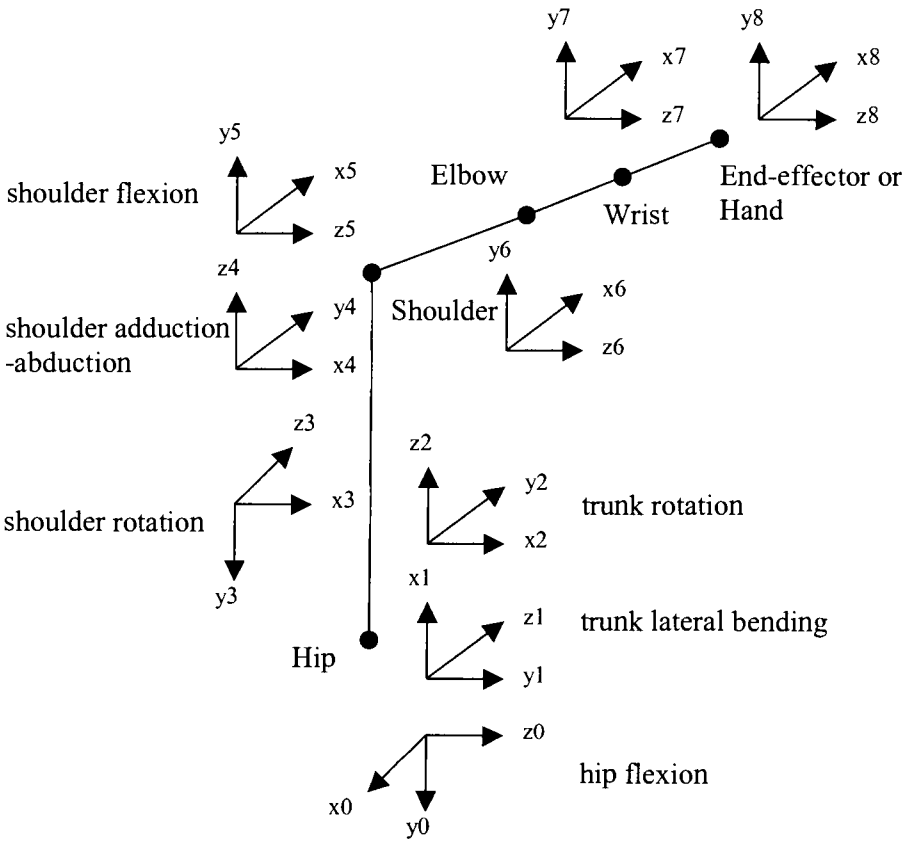

Figure 2.5: Link system of right upper limb (adapted from Jung et al., 1995).

The resolved motion method, which is a redundant manipulator technique in robotics, was found to be effective when compared to several kinematics methods for predicting human reach movement. In this method, the joint range availability was used as a performance function to guarantee kinematics optimality and to simulate human reach closely. An approximate algorithm to generate the workspaces of the human body was developed. They used the resolved motion method which determined joint velocity using a pseudoinverse matrix and then incrementally determined the joint displacements, which simulated the movement of the segments in upper limb. The trajectory of each joint between the hip and the hand were obtained. By using one subject to test the validity of the model, it showed that real reach postures were statistically similar to those obtained from the prediction model.

Dysart (1994) proposed a posture prediction model which employs a whole-body sagittal plane representation of the worker with five links which are the calf, thigh, torso, upper arm, and forearm. He used an inverse kinematic procedure as a method to calculate joint locations of postures from the inputs of the horizontal and vertical distances between the hand and ankle, the link lengths, the whole body weight, and the magnitude and direction of the load lifted.

He determined three different criteria for how humans choose postures. These criteria were defined as nonlinear objective functions included in the model. The three objective functions considered in his research were to minimize the sum

of the individual joint torques, minimize the maximum ratio of joint torque to joint strength, and to minimize the different values of torque at the ball and heel of the foot. These three objective criteria can be explained below (Dysart, 1994):

1. Total Torque:

The first objective was to minimize the sum of the individual joint torques. This investigated the theory that humans choose a posture which requires the least amount of effort which is defined as proportional to the total torque in all the joints. The objective function can be shown as follow:

$$\text{Minimize } \{|\tau_a|+ |\tau_k|+|\tau_h|+|\tau_s|+|\tau_e|\}$$

2. Percent Strength:

The second objective was to minimize the maximum ratio of torque exerted at a joint to the joint strength. The higher the ratio of torque exerted to the joint strength, the more exertion is perceived at that particular joint. Humans try to choose a posture where the overall perceived exertion is minimal. The optimal posture would be the smallest of the largest ratios of torque. The objective function was:

$$\text{Minimize } \{\text{Maximum } [(\tau_a/S_a), (\tau_k/S_k), (\tau_h/S_h), (\tau_s/S_s), (\tau_e/S_e)]\}$$

3. Balance:

The posture that humans choose is a balance condition that they assume so that they do not fall forwards or backwards. This referred to Kerk's (1992) research which investigated the stability of a posture and assumed that to prevent from falling

forwards or backwards, the amount of torque at the heel and ball must be in some criteria. The objective function was:

$$\text{Minimize } \{\tau_{ball}-\tau_{heel}\}$$

Nonlinear optimization was used to find the optimal posture which minimizes each criterion. Feasible body postures were identified based on constraints that all the joints of a posture must be within range of human motions and the posture must be stable or balanced. He used the Nelder and Mead non-linear algorithm to search for the solution. The three criteria are functions in a 3-dimensional space that have a unique minimum. The Nelder and Mead search searches in three dimensional space where a line search looks at only one dimension at a time. He claimed that the Nelder and Mead search is fast compared to other searches. However, it traded accuracy in exchange for speed.

Postures assumed by subjects performing a sagittal static lifting task were compared with the posture predicted by his three posture prediction algorithms. The observed postures showed that postures for a static lifting task could be predicted with an accuracy between 0-12 cm depending on the subject. He also found that variability of posture is higher for low hand positions compared to postures at high hand positions. Therefore, the model will be less accurate when the hand positions are low to the ground compared to higher hand positions.

However, his results did not produce an exact answer to the questions whether humans chose postures using any of the three criteria: Total Torque,

Percent Strength, and Balance. He stated that none of the postures were predicted accurately by any of these three criteria.

Jung and Choe (1996) developed a three-dimensional reach posture prediction model based on the prediction of perceived discomfort. The model predicts the posture by selecting the minimum discomfort configuration among feasible body positions to reach a target point. Discomfort is a feeling (e.g., nothing, weak, strong) at a specific posture on which external force is exerted (e.g., holding a load). The perceived discomfort rated by both the ratio and the category scales and EMG signals of six muscles were measured for the response variables of interest. The ratio scale of the perceived discomfort was measured using a magnitude estimation technique and a free modulus method. The category discomfort were divided into nine scales, for example, 0 for no perceived discomfort, 1 for just noticeable discomfort.

A regression equation was developed to determine a quantitative relationship between posture, external load, and perceived discomfort. The independent variables are the joint angles of upper body with seven degrees of freedom and the load which is the weight of the object held with a hand while discomfort is the dependent variable. The seven degrees of freedom consist of hip flexion, hip lateral bending, shoulder flexion, shoulder abduction-adduction, shoulder rotation, elbow flexion, and wrist flexion-extension. The reach posture prediction model was developed to simulate human arm reach posture. They found

that humans adopt postures of minimum discomfort among all feasible body configurations.

2.3.2. Motion Simulation

Jung and Park (1994) examined the applicability of artificial neural networks to the prediction of human reach motions. They obtained the three dimensional motion trajectories of the joints of the upper limb (shoulder, elbow, and wrist) in the right arm from 5 percentile female to 95 percentile male through a motion analysis system by investigating actual humans. The backpropagation method, which is usually used as a pattern associator, was employed as a tool for predicting such human movements. A backpropagation approach is a learning method using an algorithm which is commonly used to train networks to update the weights using the gradient search technique to minimize the mean square of the differences between the desired output vector and the actual output vector. They photographed actual human reach of ten subjects. The arm reach motions consisted of reaching for twelve distinct targets that were located in the anterior space of the subject were taken from each subject. The measured data were transformed into a network consisting of links and nodes. The network indicated the difference between the measured values and the predicted values. Predicted motions and real measurements were compared by using a pairwise t-test, and no significant

differences were found for all of the joints. Thus, it was concluded that the neural network approach can accurately simulate human reach.

Faraway (2001) developed a method for modeling the variability of motion prediction models by using the data from 20 subjects. The subjects varied in height and age so that means to assess the effects of anthropometry, gender, and age on the motions could be provided. The subjects were asked to perform hand motions to specific targets. About 8000 motions were performed by a group of 20 subjects. Using a regression model, he predicted reaching motions from information about the target of the reach and characteristics of the individual such as stature, age, and gender. The regression model had radial deviation depending on certain covariates such as the location of the target being reached, the age, and anthropometry of the subject and other factors. The radial deviation is the orthogonal distance of the hand from an axis joining the initial and final location of the hand during motion. The model can output a predicted reach for given input conditions and it can express the likely variability in that reach. For example, it can predict the amount of variability, which depends on the input conditions such as the gender of the subject.

2.4 Summary

Biomechanical models are mathematical representations of the musculoskeletal system that are developed to understand or interpret the functional behavior and joint loadings that occur during a task or exertion of interest. In biomechanical models, it is assumed that humans are likely to choose to perform tasks where they feel optimum in terms of biomechanical criteria such as minimum joint compression, maximum joint strength, or minimum fatigue.

Optimization-based models have been used to find the optimal solution to many problems in biomechanics. Posture prediction models have been developed to represent how people choose a working posture under defined conditions.

Dysart (1994) investigated postures assumed by subjects performing a sagittal static lifting task by representing the body of the worker in the sagittal plane using five links (one side of the human body), which are the forearm, upper arm, torso, thigh, and calf. Nonlinear optimization is used to determine the optimal solution which is posture that minimizes a desired objective. There are three objective functions investigated in the original model: Total Torque, Percent Strength, and Balance. However, there was no neck posture investigated in his model. So, the model could predict postures where the subject may not be able to see the load in the hands, or the neck could be fatiguing when trying to see the load.

In this thesis, a model of human body with ten links in the sagittal plane was developed. In order to predict the posture more effectively, sagittal plane of

human includes ten joints in two dimensions instead of five joints with one dimension as in Dysart's model. Thus, the model was developed to investigate both left and right sides of human parts by considering left and right ankles, left and right knees, left and right shoulders, left and right elbows, and left and right hands. In addition, the model includes the head and neck link added to the torso to determine neck posture which the eyes can see the load in the hands. Finally, the model used multi-objective optimization including both moment and balance criteria in the objective function to predict human postures.

3. MODEL DEVELOPMENT

3.1. Overview

The model applies a body plane representation of the worker with ten joints corresponding to the calves, thighs, torso, upper arms, forearms, and neck. Thus, the model developed considers both left and right sides of the body. The horizontal and vertical distances between the hands and the reference, the link lengths, the weight of each link, and the magnitude and direction of the load lift are needed as inputs to the model. The model was constructed from these inputs by using biomechanical procedures. The criterion and conditions are determined mathematically in terms of a non-linear optimization.

3.2. Overview of Posture Prediction Model

Figure 3.1 is a flowchart of how the model predicts a posture. The model employs a whole-body sagittal plane representation of the worker with ten links corresponding to the calves, thighs, torso, upper arms, forearms, and neck as shown in Figure 3.2. Inputs to the model are the horizontal and vertical distances between the hands and ankles, the link lengths and weights, and the magnitude and direction of the load lifted. With these inputs, the model calculates the joint locations of postures using kinematic procedures. A criterion was used to determine the value of variables. The criterion was defined mathematically in terms of a non-linear

objective function. The model chooses a posture by optimizing an objective function by searching a posture within a feasible solution set which is defined by three constraints: Range of Motion, Line of Sight, and Balance.

3.3. Biomechanical Model

The biomechanical model used is a ten-segment whole body lifting static model. The human body consists of the lower legs, upper legs, trunk, upper arms, lower arms, and neck. The ten joints included in the model are the neck, elbows, shoulders, hip, knees, and ankles as shown in Figure 3.2. The body's configuration at any moment is completely specified by the angles of each segment with respect to the horizontal plane. The moments of each joint can be calculated by using static biomechanical procedures with known anthropometry data.

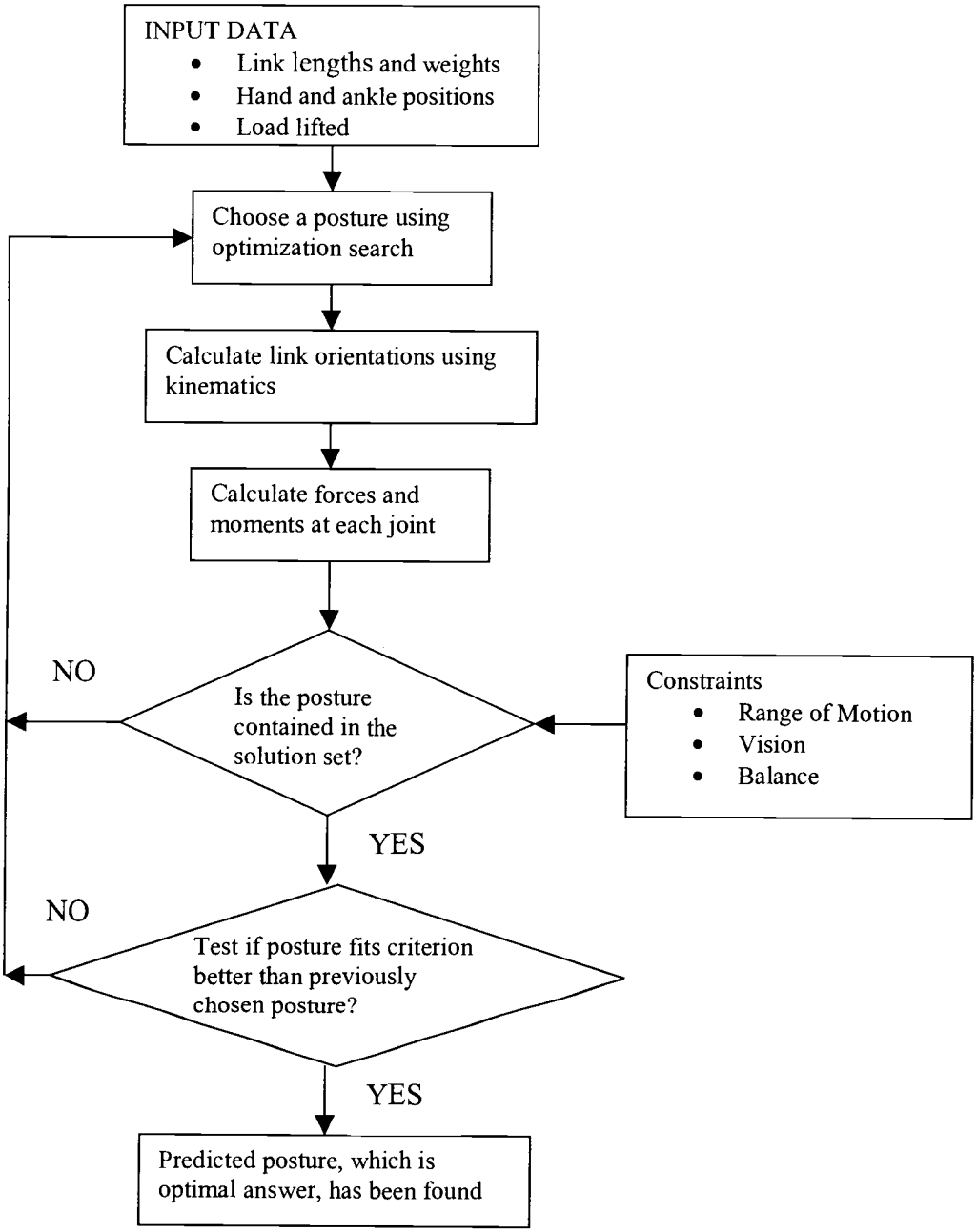

Figure 3.1: Flowchart of posture prediction model.

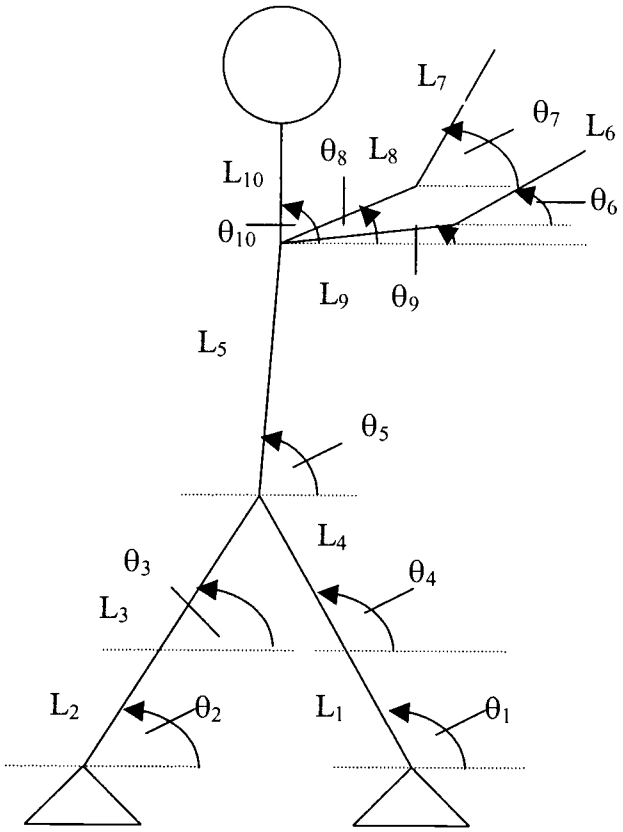

Figure 3.2: Definition of angles and joints.

3.4. Theory of Force and Moment Calculation

The methods for calculating forces and moments are adapted from Chaffin et al., (1999) by using Newtonian mechanics in his development of his planar static biomechanical models. The free-body diagram is applied to represent force vectors, which are scaled in the drawing to indicate magnitude. They can then be arranged graphically to determine the magnitude of an unknown force quantity.

3.4.1. Theory of Balance

Forces and moments at each joint are calculated by using the theory of static mechanics that when the object (which is human, in this case) is static, the summation of forces and moments must be equal to zero. It can be written in terms of two balance equations of static forces and moments in free body diagram.

1. Balance of the forces

$$\Sigma F = 0 \tag{3.1}$$

Forces are investigated in two directions: horizontal (x-axis) and vertical (y-axis). Thus, the equation (3.1) can be expressed in this form:

$$\Sigma F_x = 0 \tag{3.2}$$

$$\Sigma F_y = 0 \tag{3.3}$$

2. Balances of the moments

$$\Sigma Mo = 0 \tag{3.4}$$

where,

F = force

Mo = moment applying at a joint due to external forces and link weight

3.4.2. Variable Description

The diagram of link *i* with moment and forces applied is shown in Figure 3.2. All other variables that will be used to calculate forces and moments at each joint are described as follows:

Fx_i = the horizontal force at joint *i* due to external forces and link weight

Fy_i = the vertical force at joint *i* due to external forces and link weight

F_{XR} = the force from load applying to the right hand

F_{XL} = the force from load applying to the left hand

Mo_i = the total moment at joint *i* due to external forces and link weight.

C_i = the distance of the center of mass of link *i* relative to the orientation of joint *i*

L*i* = the length of link *i*

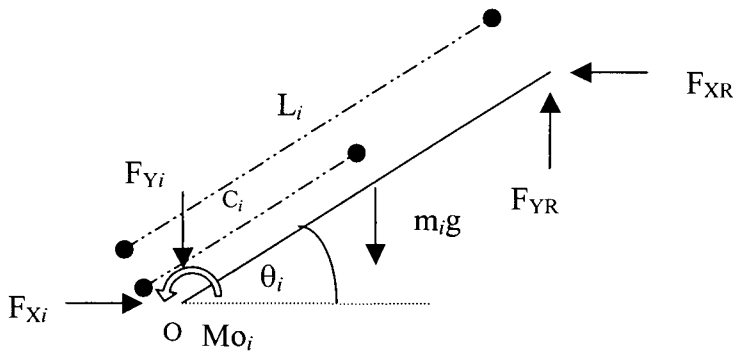

Figure 3.3: Definition of link *i*.

3.4.3. Definition of Directions

This model defined directions to calculate forces and moments as follows:

The X-axis is horizontal and positive to the right.

The Y-axis is vertical and positive in the upward direction.

Moment is positive in the counter-clockwise direction and negative in the clockwise direction (right-hand rule).

Figure 3.4 shows force and moment directions.

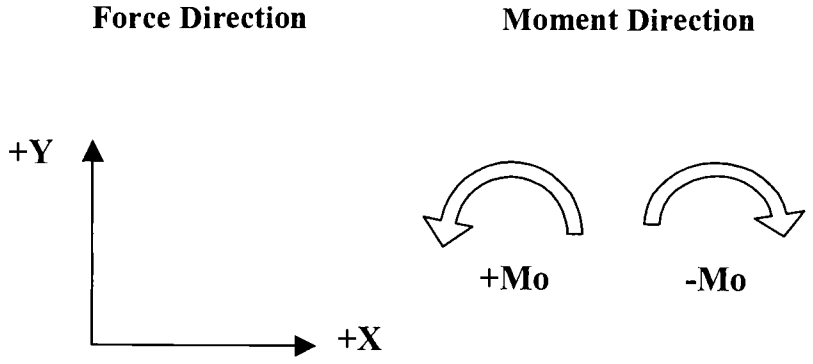

Figure 3.4: Directions of force and moment.

3.5. Calculation of Forces and Moments of Each Link

Given the hand positions, the goal is to solve for the posture. Thus, the calculations started at the hand joints where they deal with external force from the load and ended up at the feet on the floor. There is no moment at the hands because they are the positions to which external forces apply. By using the formulation described in the above section, forces and moments of each joint can be calculated. A summary of calculation of forces and moments at elbows, shoulders, hip, knees, ankles, neck, and base are presented in Table 3.1.

Table 3.1: Summation of force and moment calculations.

Link	Forces	Moments
Right Elbow (L_6)	$Fx_6 = F_{XR}$ $Fy_6 = F_{YR} - m_6g$	$Mo_6 = (m_6*g*C_6*L_6*\cos\theta_6) - (F_{XR}*L_6*\sin\theta_6) - (F_{YR}*L_6*\cos\theta_6)$
Left Elbow (L_7)	$Fx_7 = F_{XL}$ $Fy_7 = F_{YL} - (m_7*g)$	$Mo_7 = (m_7*g*C_7*L_7*\cos\theta_7) - (F_{XL}*l_7*\sin\theta_7) - (F_{YL}*l_7*\cos\theta_7)$
Right Shoulder (L_9)	$Fx_9 = Fx_6 = F_{XR}$ $Fy_9 = F_{YR} - (m_6*g) - (m_9*g)$	$Mo_9 = Mo_6 + (m_9*g*C_9*L_9*\cos\theta_9) - (Fx_6*l_9*\sin\theta_9) - (Fy_6*L_9*\cos\theta_9)$
Left Shoulder (L_8)	$Fx_8 = Fx_7 = F_{XL}$ $Fy_8 = Fy_7 - (m_8*g) = F_{YL} - (m_7*g) - (m_8*g)$	$Mo_8 = Mo_7 + (m_8*g*C_8*l_8*\cos\theta_8) - (Fx_7*l_8*\sin\theta_8) - (Fy_7*L_8*\cos\theta_8)$
Neck (L_{10})	$Fx_{10} = 0$ $Fy_{10} = -(m_{10}*g)$	$Mo_{10} = (m_{10}*g*C_{10}*L_{10}*\cos\theta_{10})$
Hip (L_5)	$Fx_5 = Fx_8 + Fx_9 + Fx_{10} = F_{XL} + F_{XR}$ $Fy_5 = F_{YL} + F_{YR} + Fy_{10} - ((m_5 + m_6 + m_7 + m_8 + m_9 + m_{10})*g)$	$Mo_5 = (Mo_8 + Mo_9 + Mo_{10}) - (Fx_8 + Fx_9 + Fx_{10})*L_5*\sin\theta_5 - (Fy_8 + Fy_9 + Fy_{10})*L_5*\cos\theta_5 + (m_5*g*C_5*L_5*\cos\theta_5)$

Table 3.1: Summation of force and moment calculations (continued).

Link	Forces	Moments
Right Knee (L_4)	$Fx_4 = (Fx_5)/2 = (1/2)(F_{XL} + F_{XR})$ $Fy_4 = (1/2)(F_{YL} + F_{YR} - (m_5 + m_6 + m_7 + m_8 + m_9 + m_{10})*g) - (m_4*g)$	$Mo_4 = (Mo_5/2) - (Fx_5/2)*L_4*\sin(180-\theta_4) + (Fy_5/2)*L_4*\cos(180-\theta_4) - (m_4*g*C_4*l_4*\cos(180-\theta_4))$
Left Knee (L_3)	$Fx_3 = (Fx_5)/2 = (1/2)(F_{XL} + F_{XR})$ $Fy_3 = (1/2)(F_{YL} + F_{YR} - (m_5 + m_6 + m_7 + m_8 + m_9 + m_{10})*g) - (m_3*g)$	$Mo_3 = (Mo_5/2) - (Fx_5/2)*L_3*\sin(\theta_3) - (Fy_5/2)*L_3*\cos(\theta_3) + m_3*g*C_3*L_3*\cos(\theta_3)$
Right Ankle (L_1)	$Fx_1 = Fx_4 = (1/2)(F_{XL} + F_{XR})$ $Fy_1 = (1/2)(F_{YL} + F_{YR} - (m_5 + m_6 + m_7 + m_8 + m_9 + m_{10})*g) - (m_4*g) - (m_1*g)$	$Mo_1 = Mo_4 - Fx_4*L_1*\sin(180-\theta_1) + Fy_4*L_1*\cos(180-\theta_1) - m_1*g*C_1*L_1*\cos(180-\theta_1)$
Left Ankle (L_2)	$Fx_2 = Fx_3 = (Fx_5)/2 = (1/2)(F_{XL} + F_{XR})$ $Fy_2 = (1/2)(F_{YL} + F_{YR} - (m_5 + m_6 + m_7 + m_8 + m_9 + m_{10})*g) - (m_3*g) - (m_2*g)$	$Mo_2 = Mo_3 - Fx_3*L_2*\sin(\theta_2) - Fy_3*L_2*\cos(\theta_2) + m_2*g*C_2*L_2*\cos(\theta_2)$

All complete calculations of each joint are described in Appendix A. Below is the example of how to calculate the force and moment at right elbow, which is the first link in calculation.

Assume that we have a 100 N force acting to the right hand in the x direction as shown in Figure 3.5. The weight of right elbow is 14.06 N and the center of mass is 0.39 m from the elbow. The elbow has a rotate position of 30° from horizontal with the link length of 0.253 m. All information for calculation the force and moment at the right elbow are summarized below.

Given $F_{XR} = 100$ N, $F_{YR} = 0$ N, $m_6g = 14.06$ N, $C_6 = 0.39$ m, $L_6 = 0.253$ m, $\theta_6 = 30°$

Right Elbow (L_6):

Forces:

$$\Sigma F = 0 \tag{3.5}$$

Thus, the summation of forces in the x-direction must be equal to zero as well as in the y-direction.

From the free-body diagram shown in Figure 3.5, there are two forces in the x-direction. The equations can be written as follows:

$$\Sigma Fx = 0 \tag{3.6}$$

$$Fx_6 - F_{XR} = 0 \tag{3.7}$$

In order to find the value of Fx_6, equation (3.7) can be rewritten as:

$$Fx_6 = F_{XR} = 100 \tag{3.8}$$

On the other hand, there are three forces in the y-direction. The equations can also be expressed as follows:

$$\Sigma Fy = 0 \tag{3.9}$$

$$F_{YR} - Fy_6 - m_6 g = 0 \tag{3.10}$$

Thus,

$$Fy_6 = F_{YR} - m_6 g = 0 - 14.06 = -14.06 \text{ N} \tag{3.11}$$

Moments:

From the free-body diagram shown in Figure 3.5, the moment equations can be expressed as follows:

$$\Sigma Mo_{\text{right-elbow}} = 0 \tag{3.12}$$

$$Mo_6 - (m_6 * g * C_6 * L_6 * \cos\theta_6) + (F_{XR} * L_6 * \sin\theta_6) + (F_{YR} * L_6 * \cos\theta_6) = 0 \tag{3.13}$$

$$Mo_6 = (m_6 * g * C_6 * L_6 * \cos\theta_6) - (F_{XR} * L_6 * \sin\theta_6) - (F_{YR} * L_6 * \cos\theta_6) \tag{3.14}$$

$$= (14.06 \times 0.39 \times 0.253 \times \cos 30°) - (100 \times 0.253 \times \sin 30°)$$

$$- (0 \times 0.2526 \times \cos 30°)$$

$$= -11.43 \text{ N-m}$$

In conclusion, the force at the right elbow is the combination vector of the forces 100 N in +X direction (the same direction of F_{X6} in Figure 3.5) and 14.06 N in +Y direction (the opposite direction of F_{Y6} in Figure 3.5). The moment at the right elbow joint has the magnitude of 11.43 N-m in clockwise direction.

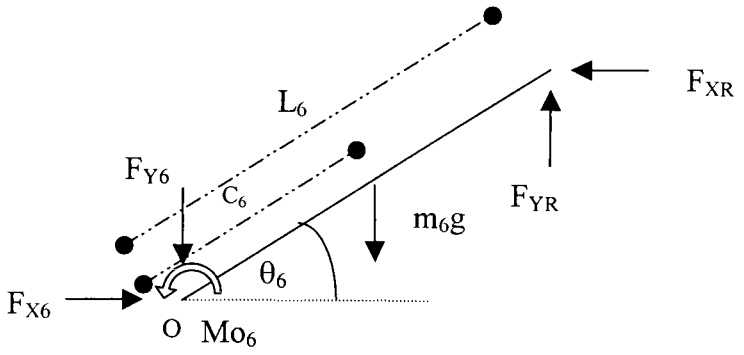

Figure 3.5: Free body diagram of right elbow.

3.6. Calculation of Forces and Moments at the Heel and Ball of the Foot

Moments at the heel and ball of feet are calculated by using Kerk's (1992) stability equations. His assumptions in terms of balance include:

1. The body will not fall backward if the moment taken about the heel of the foot is less than or equal to zero ($M_{heel} < 0$). The moment at heel is calculated by assuming that there is no reaction force at the ball.
2. The body will not fall forward if the moment taken about the ball of the foot is greater than or equal to zero ($M_{ball} \geq 0$). The moment at ball is calculated by assuming that there is no reaction force at the heel.

These criteria use the moment levels at the ball and heel of the foot shown in Figure 3.6, which will be discussed in Appendix A.

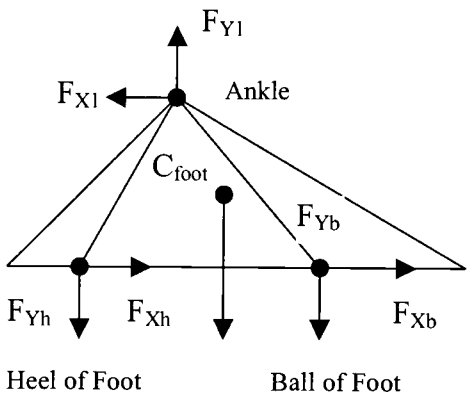

Figure 3.6: Forces at the foot.

3.7. Optimization Model

The calculation in the above sections will be modeled in the form of an optimization model. The posture prediction optimization model developed in this thesis is a nonlinear programming model. It has a nonlinear objective function and consists of both linear and nonlinear constraints and the objective function is minimized. The objective function and constraints are presented in the following sections.

3.7.1 Objective Function

The objective function formulated is a multi-criteria objective function. The two criteria modeled in the objective function are: 1) the sum of the squared moments about the joints, and 2) balance, which is modeled as the square of the sum of the moments about the ball and heel of the feet. The objective function is a convex combination of these two criteria. The two criteria are discussed next.

3.7.1.1. Sum of the squared moment about the joints

This criterion represents the idea of putting a higher loading on the weaker upper torso joints. The more torque at each joint, the less amount of effort from the human. Effort is defined as proportional to the total square of moment in all the joints, thus, this criterion also investigates the theory that humans choose a posture that requires the least amount of effort. The model using the squared torque objective function was able to come reasonably close to the observed posture, especially for the two higher hand positions (Woldstad, 1996).

This equation to minimize the sum of the squared moment at the joint is shown below.

$$\text{Minimize } \{Mo_1^2 + Mo_2^2 + Mo_3^2 + Mo_4^2 + Mo_5^2 + Mo_6^2 + Mo_7^2 + Mo_8^2 + Mo_9^2 + Mo_{10}^2\}$$

Where,

Mo_1, Mo_2 are moments at the right and left ankle, respectively.

Mo_3, Mo_4 are moments at the left and right knee, respectively.

Mo_5 is the moment at the hip.

Mo_6, Mo_7 are moments at the right and left elbow, respectively.

Mo_8, Mo_9 are moments at the left and right shoulder, respectively.

Mo_{10} is the moment at the neck.

Since there is no motion, static moment theory is used to calculate forces and moments in the objective function. The static moment calculation is adapted from Chaffin (1999).

The following equation shows an example of moment formula at the right elbow from the previous example.

$$Mo_6 = (m_6*g*C_6*L_6*\cos\theta_6) - (F_{XR}*L_6*\sin\theta_6) - (F_{YR}*L_6*\cos\theta_6) \quad (3.15)$$

$$= (14.06 \times 0.39 \times 0.253 \times \cos30°) - (100 \times 0.253 \times \sin30°)$$

$$- (0 \times 0.2526 \times \cos30°)$$

$$= -11.43 \text{ N-m}$$

3.7.1.2. Balance

This criterion explains the chosen posture in favor of balance. Humans choose a posture in which they feel comfortable to stand. A balanced posture allows a person to be able to remain standing. Thus, the chosen posture will be one in which the human does not feel like falling forwards or backwards. This criterion can be defined as:

$$\text{Minimize } (Mo_{hl} + Mo_{bl} + Mo_{hr} + Mo_{br})^2$$

Where,

Mo_{hl} is the moment at the heel of the left foot.

Mo_{bl} is the moment at the ball of the left foot.

Mo_{hr} is the moment at the heel of the right foot.

Mo_{br} is the moment at the ball of the right foot.

3.7.2. Constraints

A set of constraints was used to restrict postures to those that are both feasible (from a physiological standpoint) and practical (from a human factors standpoint). The constraints in this model can be categorized as follows:

3.7.2.1. Constraints related to the human body

All the angles of joints for posture must be within the defined joint range of motion. The joint mobility or range-of-motion constraints specify the upper and lower bounds for the included angle of each joint. Each link angle is checked to ensure that it is feasible for humans by being in the range of motion values shown in the Table 3.2 and definition of angles provided in Figure 3.7.

Table 3.2: Constraints on each joint range of motion (adapted from Web Associates, 1978).

θ	Lower	Upper
θ_a	29°	153°
θ_k	0°	174°
θ_h	50°	-180°
θ_s	120°	370°
θ_e	0°	180°

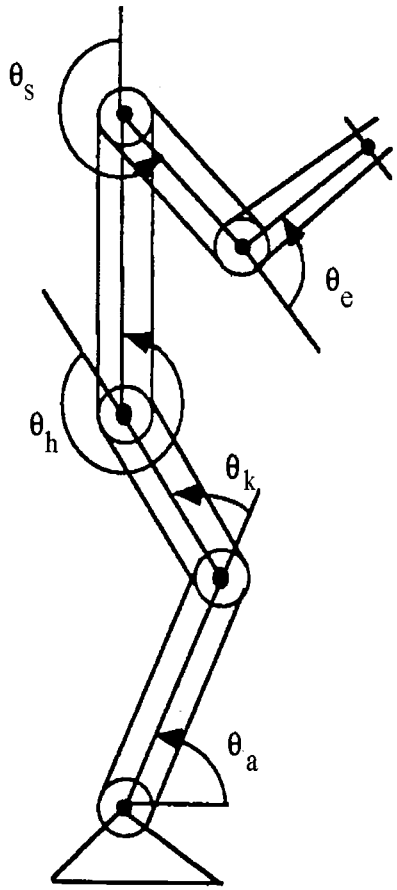

Figure 3.7: Definition of angles (adapted from Dysart, 1994).

3.7.2.2. Constraints related to the hip

The hip joint must be inside the feasible region, which means that the sum of each leg length must be equal.

3.7.2.3. Constraints related to the hands

The hands in the model will be placed at a specific position. The maximum reach distance is the distance between the back of the shoulder to the finger tips. These constraints ensure that the reach distance of each hand will not be greater than the sum of its arm length.

3.7.2.4. Constraints related to the feet

The model must predict a posture with both feet on the floor.

3.7.2.5. Constraints related to balance

Humans should stand in the posture in which they feel stable without tipping forwards or backwards. The balance constraints in this thesis are adapted from Kerk's (1992) stability constraints. He stated that if the amount of torque at the heel or ball exceeds a certain limit, the body will not be stable, consequently falling forwards or backwards.

The balance assumptions can be categorized by the following:

1. If the torque at the heel of the back foot is less than or equal to zero, it is assumed that the body will not tip backwards.
2. If the torque at the ball of the front foot is greater than or equal to zero, it is assumed that the body will not tip forwards.

Balance constraints ensure the stability of a predicted posture while the balance criteria in the objective function investigate the theory that humans choose a posture in which they are most stable. Thus, people choose a posture that they will not fall forwards or backwards.

3.7.2.6. Constraints related to the line-of-sight vision

The visual demands of a task and the location of visual displays are important not only in themselves, but also because they largely determine the posture of the head and neck (Pheasant, 1986).

This thesis includes the head and neck link, and line-of-sight vision constraints. These constraints ensure that the model will predict a posture where the subject can see the load held in the hands, and which is not fatiguing to the neck. The hands must be within the range of a 34 degree visual cone in front of the eyes. This visual cone can extend up to 10 degrees above the vector perpendicular to the neck and 24 degrees below this vector (Pheasant, 1986). Neck Posture is

determined by the algorithm to consider line of sight by keeping the hand within this 34 degree visual cone.

The diagram of head posture for neck extension and flexion is shown in Figure 3.8.

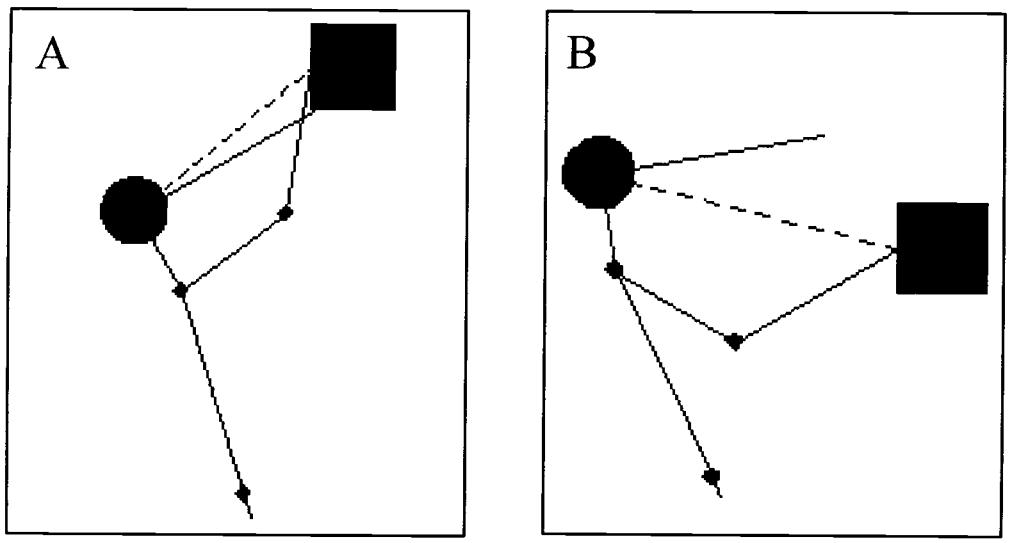

Figure 3.8: The estimated head posture for neck extension and flexion (adapted from Woldstad, 1996).

3.8. Summary

The model developed in this thesis applies a body plane representation of the worker with ten joints corresponding to the calves, thighs, torso, upper arms, forearms, and neck. The model considers both left and right sides of the body as it has different links defining the left side and right side of the human parts. In other words, the side consists of the left upper arm, left forearm, left thigh, and left calf while the right side consists of the right upper arm, right forearm, right thigh, and right calf. Line of sight is also considered in the model to make sure that the model can predict a position in which the human can see the load. Model constraints ensure that the predicted postures are feasible and practical. The model uses multi-objective function consisting of total squared moments and balance as criteria to predict a posture. Optimization model with a multi-objective function and sets of constraints are summarized below.

Objective function:

Minimize $f(x_1) + f(x_2)$

Where $f(x_1)$ is the function of sum of the squared moments criteria and f(x2) is function of balance criteria.

$$f(x_1) = (Mo_1)^2 + (Mo_2)^2 + (Mo_3)^2 + (Mo_4)^2 + (Mo_5)^2 + (Mo_6)^2 + (Mo_7)^2 + (Mo_8)^2 + (Mo_9)^2 + (Mo_{10})^2$$

$$f(x_2) = (Mo_{br} + Mo_{hr} + Mo_{bl} + Mo_{hl})^2$$

Therefore, the objective function can be rewritten below.

Minimize $(Mo_1)^2 + (Mo_2)^2 + (Mo_3)^2 + (Mo_4)^2 + (Mo_5)^2 + (Mo_6)^2 + (Mo_7)^2 + (Mo_8)^2 + (Mo_9)^2 + (Mo_{10})^2 + (Mo_{br} + Mo_{hr} + Mo_{bl} + Mo_{hl})^2$

Constraints:

- Constraints related to the human body
- Constraints related to the hip
- Constraints related to the hands
- Constraints related to the feet
- Constraints related to balance
- Constraints related to line-of-sight vision

From the criteria and constraints described in the above sections, a posture prediction model is formulated and shown in Appendix B.

4. SIMULATION RESULTS

4.1. Overview

This chapter demonstrates how the model developed in chapter 3 predicts a posture. First, this chapter describes the parameters, which were used in the model. Secondly, the techniques to solve for the optimum posture are explained. The results of some predicted postures are then investigated.

4.2. Simulation Parameters

The model uses hand positions and load magnitude with direction as an input. Furthermore, the calculation for output is determined by using information of link lengths, center of mass position, and some foot anthropometry as constants.

Table 4.1 shows link lengths and center of mass (COM) positions that were used in this thesis. Link lengths and COM from proximal ends in Table 4.1 were adapted from Roebuck et al., (1975).

Table 4.1: Link lengths and COM positions.

Link	Link Length (m)	COM Position (m)
Hand	0.186869224	0.03363646
Forearm	0.252619506	0.098521608
Upper Arm	0.32183033	0.165098959
Neck/Head	0.314909248	0.146747709
Torso	0.498317931	0.189360814
Thigh	0.423916295	0.157696862
Shank	0.425646566	0.157914876
Foot_Heel	0.021829094	0.115720497
Foot_Toe	0.174106748	0.147280633

Weights of each link are shown in Table 4.2. These segment weights were adapted from Roebuck et al., (1975).

Table 4.2: Segment weights.

Link	Link Weight (N)
Hand	6.151553737
Forearm	14.06069426
Upper Arm	22.84862817
Neck/Head	64.15191755
Torso	445.5482493
Thigh	90.51571928
Shank	37.78811582
Foot	13.18190087

Foot anthropometry was based on Pheasant (1986) and Kerk (1992). Table 4.3 and Figure 4.1 show foot anthropometry used in this thesis.

Table 4.3: Foot anthropometry data.

Foot Anthropometry	
Foot Height (y)	0.069432298
Foot Length (front, x)	0.208296895
Foot Length (back, x)	0.054704235
Foot Length (total, x)	0.26300113
Ankle-Ball	0.189360814
Toe-Ball	0.034190147
Ball-Heel	0.195935842
Ankle-COM (x)	0.061016262
Ankle_x	-0.208296895
Ankle_y	0.069432298

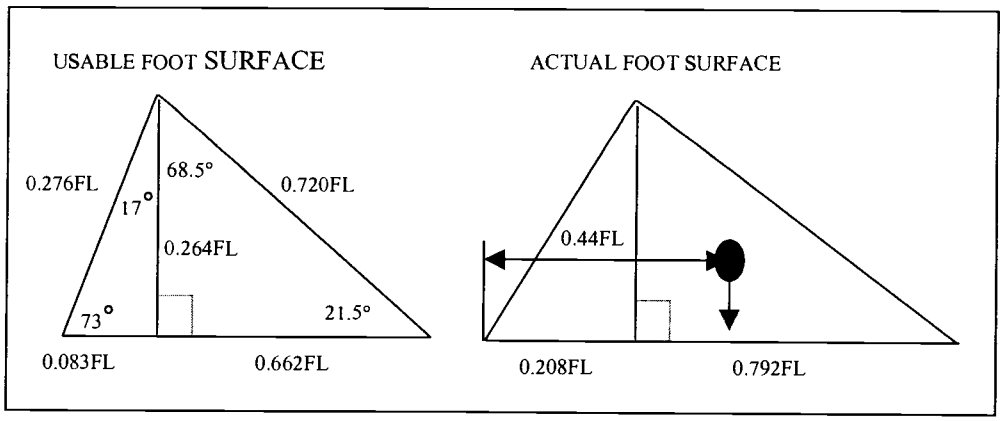

Figure 4.1: Foot anthropometry.

4.3. Software Application

From the posture prediction model developed in previous chapter, one can predict the optimum posture by using hand load and hand position as inputs. The predicted posture will be in terms of ten angles relative to horizontal of body segments: neck, elbows, shoulders, hip, knees, and ankles. The appropriate software application was chosen to solve the model, which is a nonlinear optimization model. The model in this thesis uses "Lingo6" software package as a tool to solve the problem and Excel (version 2000) as an interface to the users. Lingo is a tool designed to make building and solving linear and nonlinear optimization models faster. A user interface was also developed in Excel to provide users with a convenient way to access the data. Instead of dealing with the data directly in the Lingo program, users can input information of hand load and hand position into the Excel file. This information will be used in calculations when the users solve the model in the Lingo program. After the model is solved, the output of postural information: degrees of neck, elbows, shoulders, hip, knees, and ankles, and graphical posture will be shown in the Excel interface. All the codes of the model in Lingo program are shown in Appendix C.

4.4. Experimental Method

The experimental task was performed by inputs of three different hand positions (1.5 m, 1 m, 0.5 m). There were eight different load directions applying to the hands at each hand position. The combination of all hand load directions and positions can be shown in Table 4.4.

Table 4.4: Combination of hand loads and hand positions applied to the model.

Hand Position (Y) (meters)	Direction Of Force (100 N)	Hand Position (Y) (meters)	Direction of Force (100 N)	Hand Position (Y) (meters)	Direction Of Force (100 N)
1.5	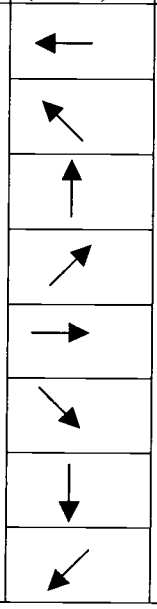	1	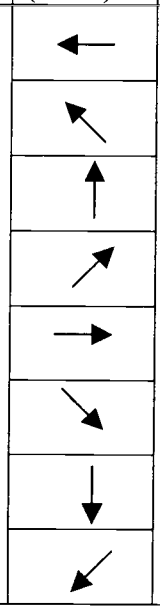	0.5	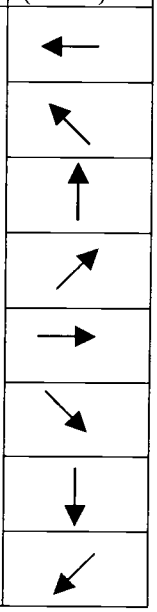

From Table 4.4, both left hand and right hand were assumed in the same height of position at each hand position. All forces represent reaction forces from the load which were in the opposite directions of the action to loads. The magnitude of reaction force is equal to 100 N in each case.

Postures at each combination of force direction and hand position were predicted and shown in Figure 4.2, Figure 4.3, Figure 4.4, Figure 4.5, Figure 4.6, and Figure 4.7. The complete details of the predicted postures are shown in Appendix D.

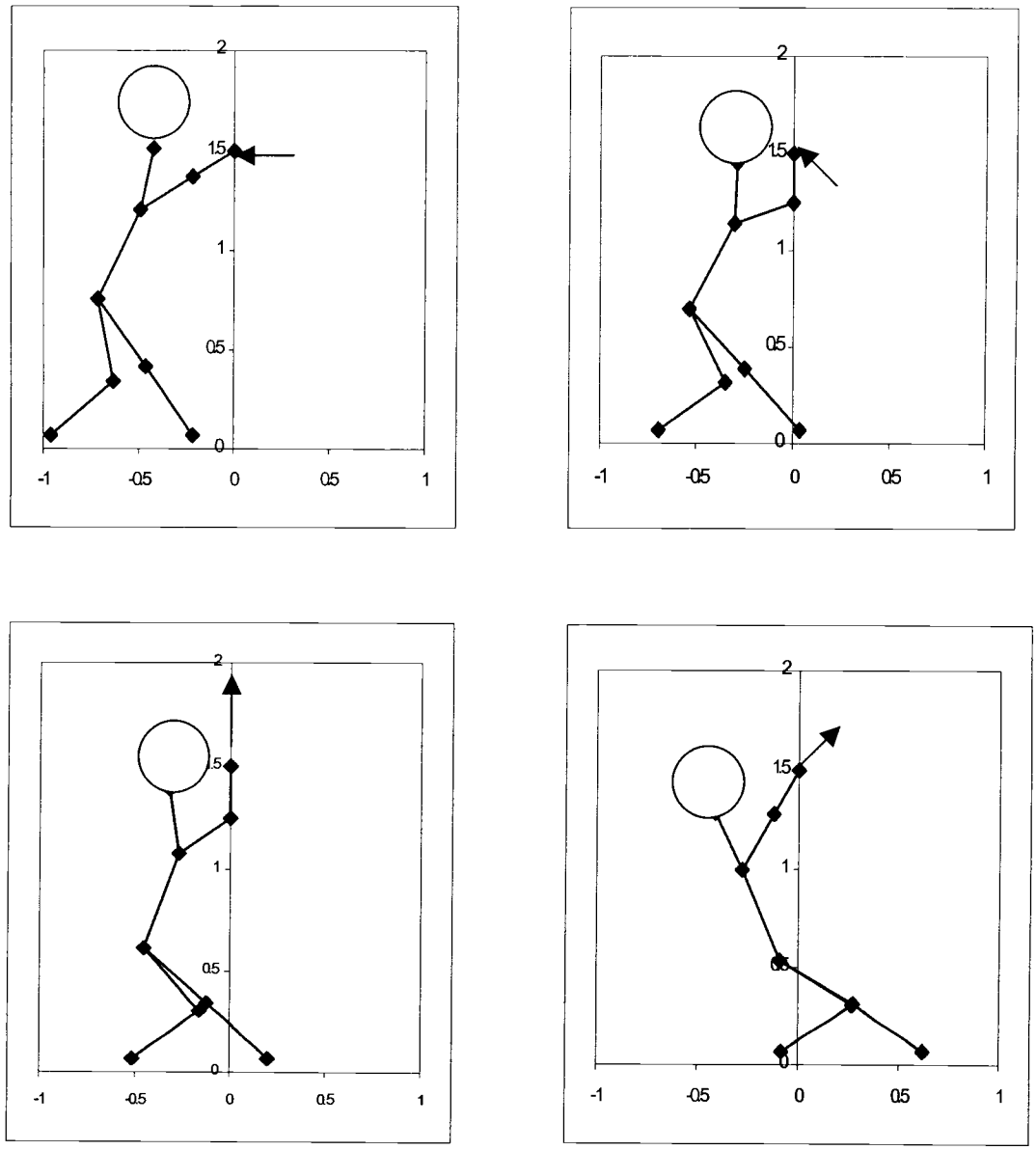

Figure 4.2: Predicted postures at hand position of 1.5 meters with different load directions.

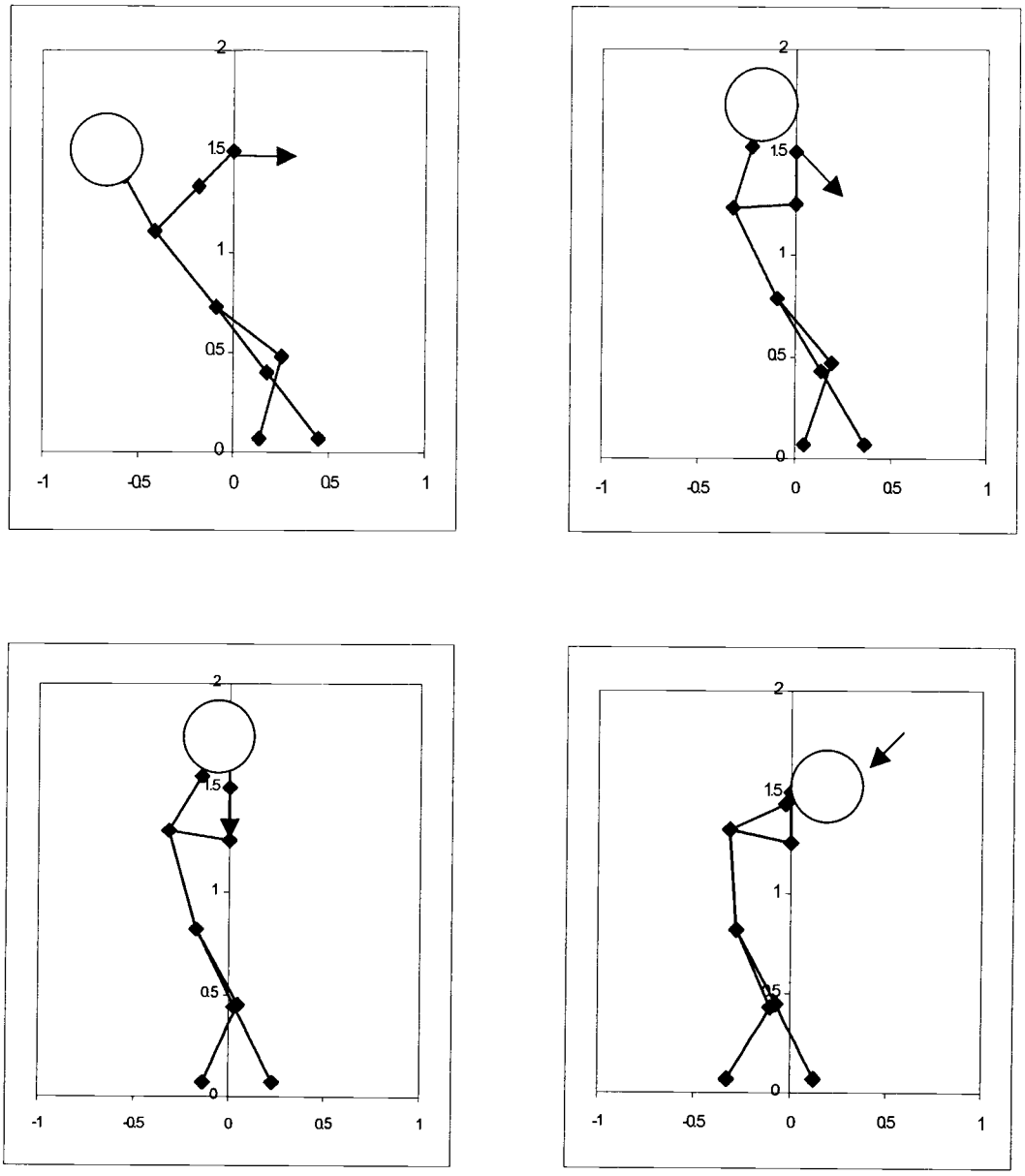

Figure 4.3: Predicted postures at hand position of 1.5 meters with different load directions (continued).

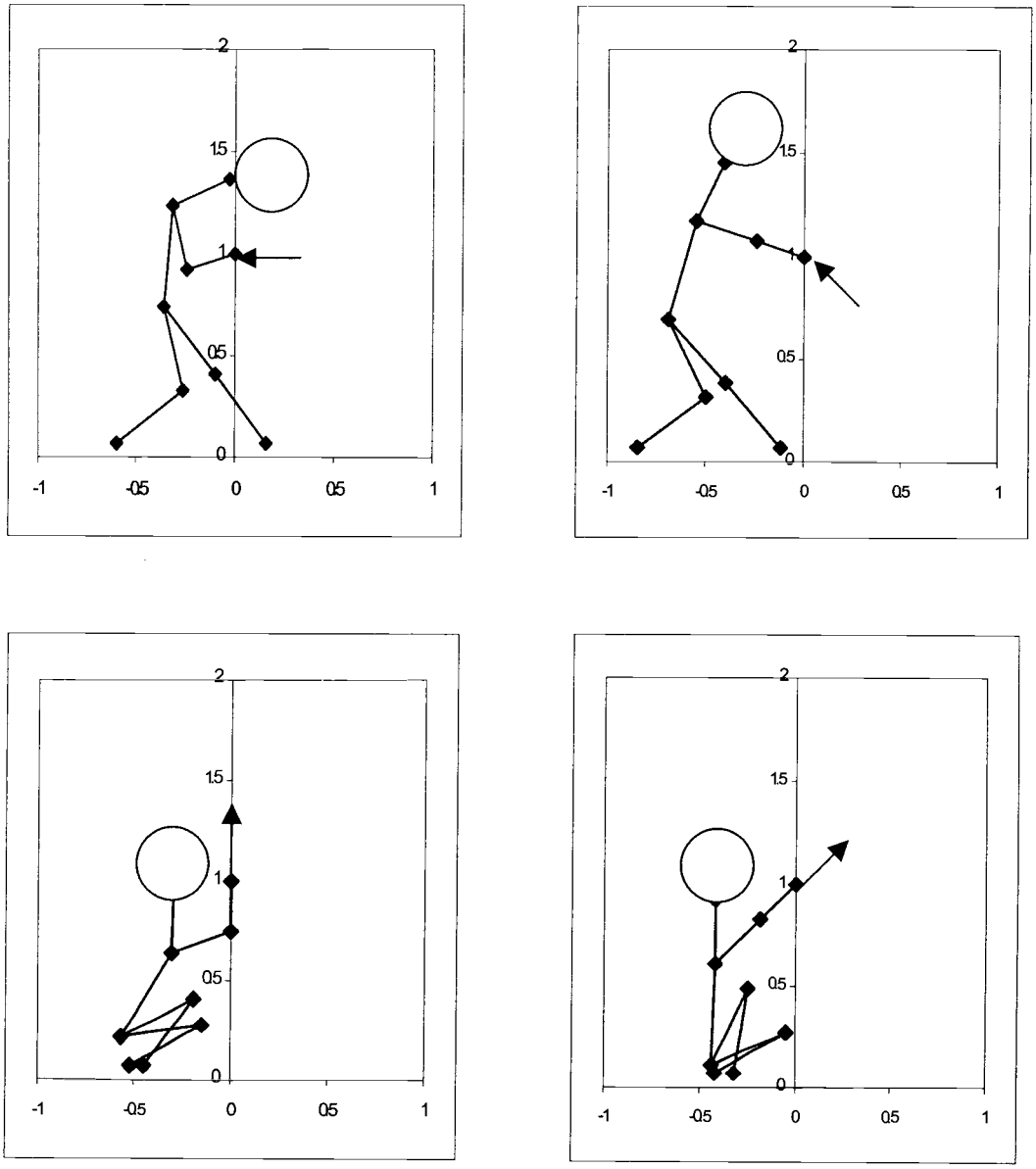

Figure 4.4: Predicted postures at hand position of 1.0 meter with different load directions.

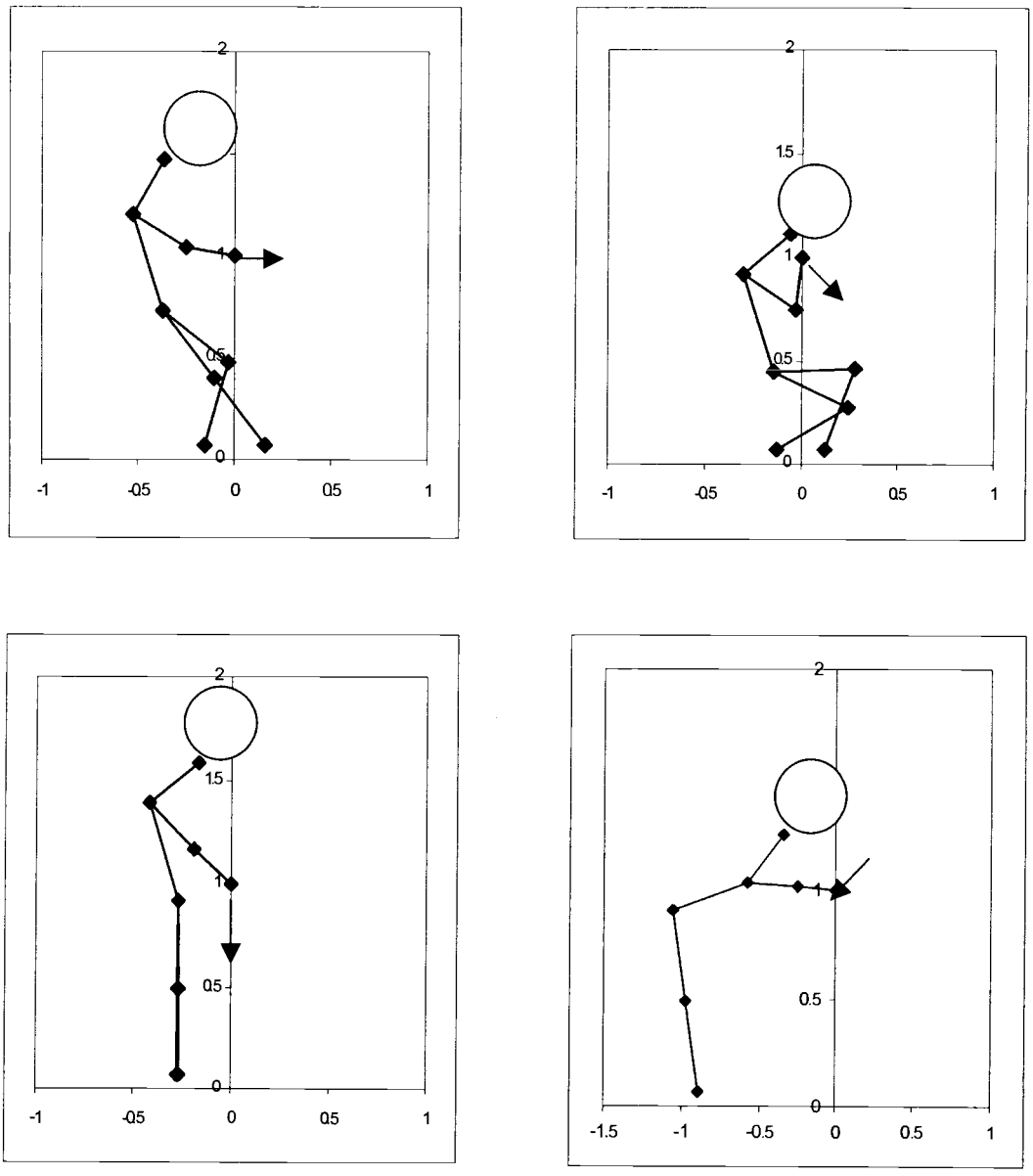

Figure 4.5: Predicted postures at hand position of 1.0 meter with different load directions (continued).

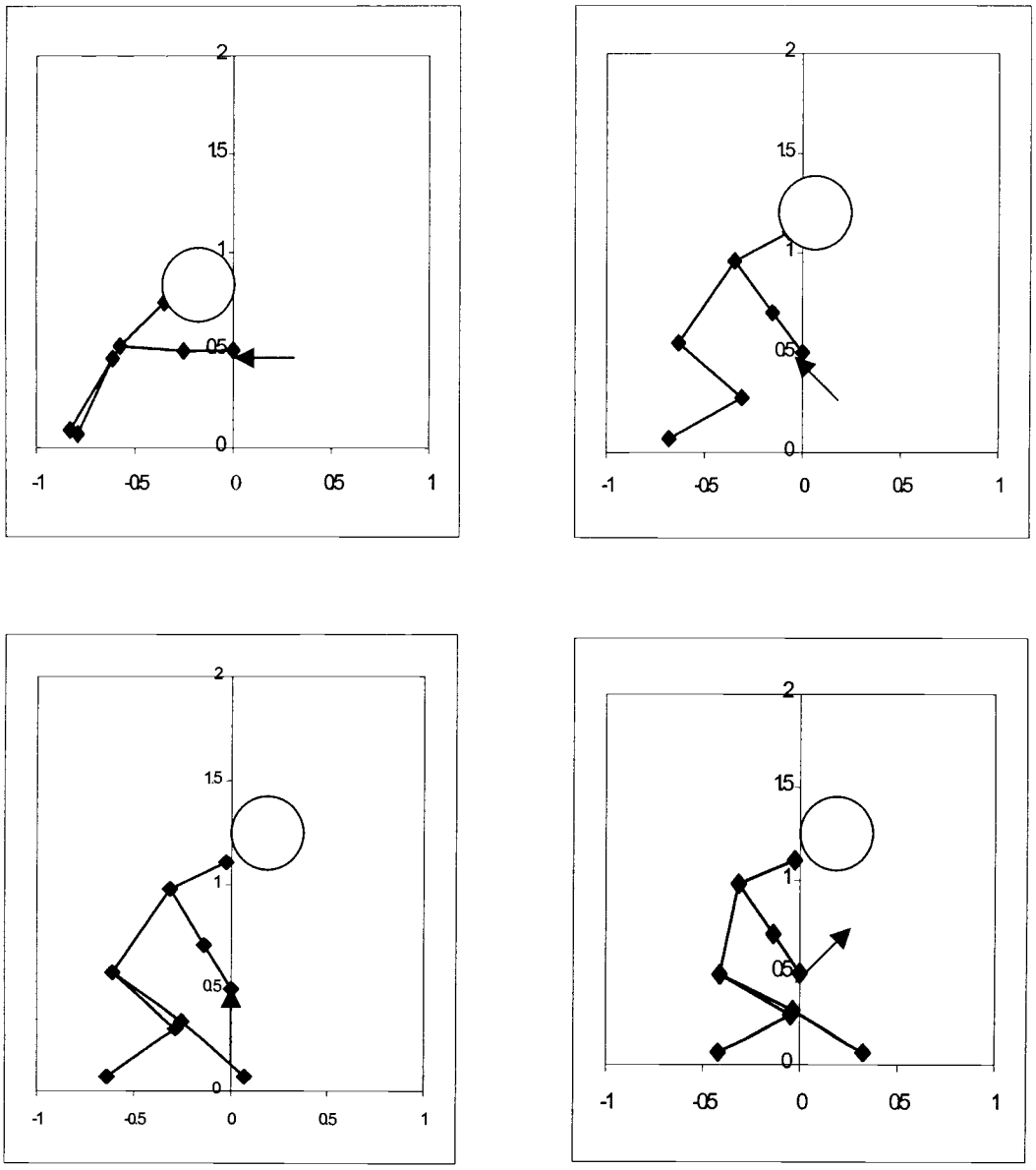

Figure 4.6: Predicted postures at hand position of 0.5 meter with different load directions.

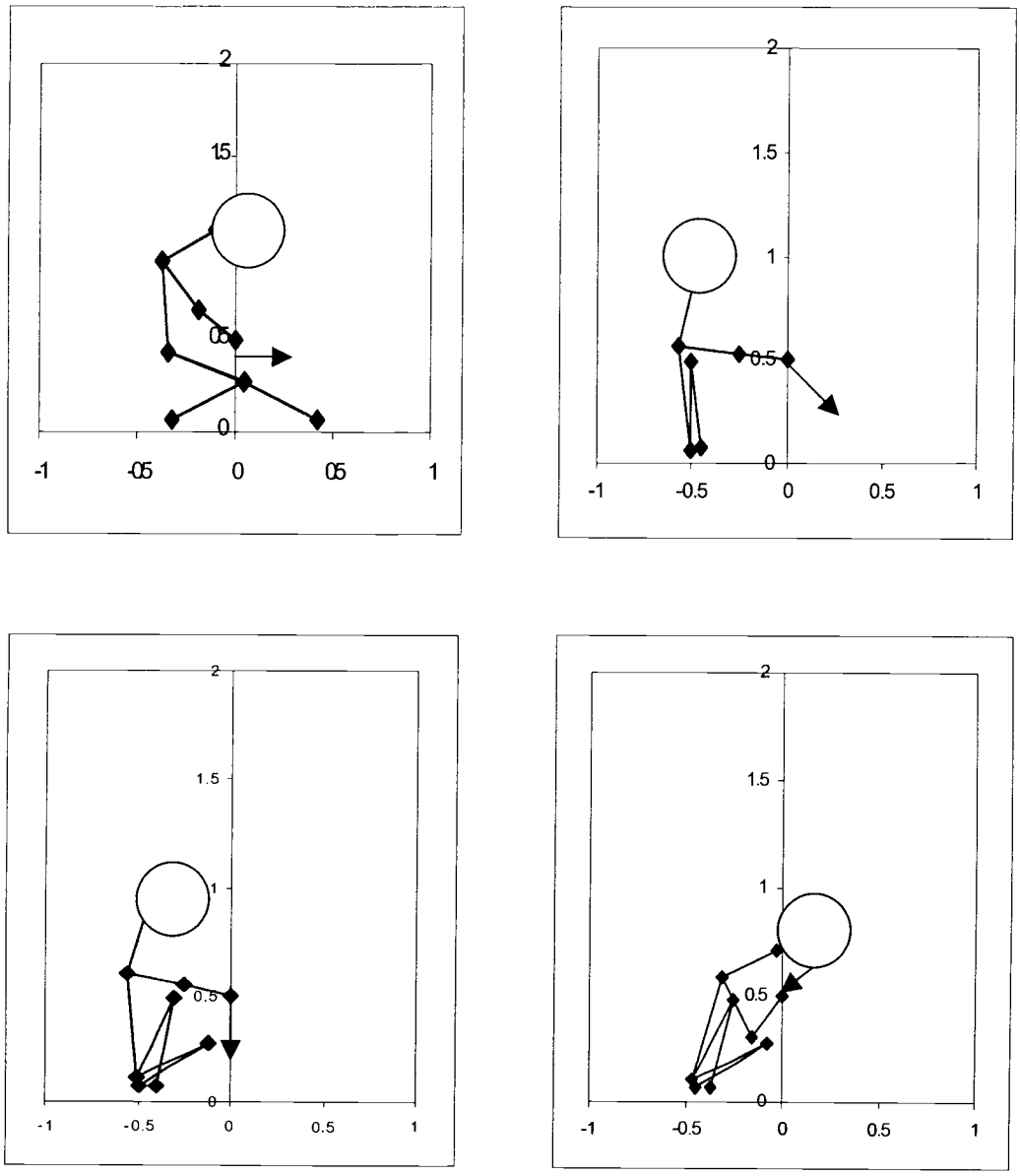

Figure 4.7: Predicted postures at hand position of 0.5 meter with different load directions (continued).

5. DISCUSSION

This chapter discusses the model and the results obtained with regards to each of the objectives listed in chapter 1. In addition, a discussion of research is provided which could contribute to the accuracy of posture prediction.

5.1. Discussion of the Objectives and Results

The first objective of this thesis was to develop a model representing two sides (left and right) of the human body and predict a posture from information of the load and the distance between the hands and the floor. From these input, the model predicts a posture associated with a work task. The model ensures that a predicted posture is feasible in terms of biomechanical criteria: range of motion, balance, and visible hand position. The prediction posture can be used as a base reference for inputting into other biomechanical models. By predicting posture from the model, one can obtain postures of the workers without direct measurement of postures from the workers, which can be expensive and time consuming.

The second objective was to include the moment and balance criteria in the objective function. Dysart (1994) found that none of the postures in his experiment were predicted accurately by any of these criteria. Therefore, the use of multi-objective function in this thesis by considering both moment and balance

simultaneously as criteria of how a human chooses a posture should improve the accuracy of the predicted posture.

The third objective was to demonstrate the application of the model in predicting a posture, which was done in Simulation Results. Since the model applies to both left and right sides of the human body, the accuracy of the prediction should be improved from Dysart's model which has one dimension (one side) of the human body. However, by using results from the model, one must be aware of the difference between the predicted and actual postures. The result postures can be further justified the accuracy of prediction in a future research. Fortunately, Dysart (1994) found that the variability of human posture is higher for low hand positions compared to postures at high hand positions. If we assume that the accuracy of the posture prediction model will be affected in a similar way, the accuracy of the model may be less accurate when the hand positions are low to the grounds. An example of low position is when the hands are working at a height closed to the knees; high position conversely is when the hands are held in the area of the chest and shoulder.

One of the limitations of this model was that the forces and moments were divided equally when they were distributed to the left and right adjacent joints. For example, if the moment generated at the hip is 100 N-m, the moments distributed to the left and right thighs will be assumed to be 50 N-m at each. This assumption

may not be the best. Further criteria could be investigated to find the appropriate weight to distribute the forces and moments.

From the findings, the distance between the eyes and the hands were closer for the postures predicted at the height of 1.5 m and 1.0 m than those predicted at the height of 0.5 m. Thus, the distance between eyes and hands should be considered to ensure the appropriate visibility of the hands (i.e., the hands should not be too closed to the eyes).

Furthermore, this thesis uses the specific anthropometry data in calculation for results of predicted postures so one must consider the variability between the anthropometry of the worker and reference anthropometry, which is used in calculation. The variability between those data can lead to errors in prediction.

5.2. Future Research

This section describes future research, which can be done in order to improve the understanding of human posture prediction and develop more accurate posture prediction model.

5.2.1. Validating the Predicted Posture from the Model

In order to validate the postures from a model, future research should include an experiment performed by human subjects to compare predicted postures,

and actual postures of workers. The data should come from an appropriate method in consideration of factors such as measurement, subject variability, and take into account statistical errors. The observed posture should be compared with the predicted postures from the computer model. Evaluation of the data comparing the actual human postures and predicted posture from the model will allow researchers to develop a statistical method to justify the model accuracy.

5.2.2. Developing a Non-Linear Search Method for Optimization

The model in this thesis uses "Lingo" which is optimization software to find an optimal answer. Calculations were fast because it took only a few seconds compared to non-linear search method from Dysart's model, which took 5 to 25 minutes to predict a posture. However, in order to obtain the most optimal answer from the model, a more effective non-linear method can be developed for finding the optimal solution that should be the global optimum instead of local optimum. Further analyses focusing on search algorithm for non-linear optimization model can be implemented. In addition, future research can compare the results from different algorithms used to find the solutions to ensure the truly minimum answers.

5.2.3. Developing a Three-Dimensional Posture Prediction Model

Since the model in this thesis considered human in two dimensions, another model with three dimensions should be developed for more accurately predicted postures. Since human can actually posture in many different ways, a model with three dimension representational of the human body should be better in results as it is similar to human because it has more details of human posture.

5.2.4. Considering Other Biomechanical Factors that Influence Posture

Additional research should investigate other factors that influence how humans choose a posture. Besides moment of joint and balance that were included in the objective function of the model, it is possible that there are more factors affecting posture criteria, for example, joint strength. These criteria could be included together in the model with appropriate weights. This thesis did not include the strength of the joint as one of the criteria in multi-objective function. Because the joints have both flexion and extension, they affect the sign of joint strengths and make it impossible to include joint strengths mathematically in the model at this time.

Moreover, the posture at each joint depends on the characteristics of ligaments, tendons, and fatigue. These factors should be considered in future research for more accurate prediction.

BIBLIOGRAPHY

Abdel-Malek, K., Yu, W., & Jaber, M. (2001). Realistic posture prediction. SAE Digital Human Modeling and Simulation.

Anderson, C.K., Chaffin, D.B., & Herrin, G.D. (1986). A study of lumbosacral orientation under varied static loads. Spine, 11 (5), 456-462.

Armstrong, T.J., & Chaffin, D.B. (1978). Some biomechanical aspects of the carpal tunnel. Journal of Biomechanics, 12, 567-570.

Beale, E.M.L. (1988). Introduction to optimization. New York: John Wiley and Sons.

Bean, J.C., & Chaffin, D.B. (1988). Biomechanical model calculation of muscle contraction forces: A double linear programming method. Journal of Biomechanics, 21 (1), 59-66.

Brinckmann, M., & Hilwed, D. (1988). Fatigue fracture of human lumbar vertebrae. Clinical Biomechanics, 3, S1-S23.

Byun, S. (1991). Development of a multivariate biomechanical posture prediction model using inverse kinematics. Doctoral dissertation, University of Michigan, Ann Arbor, MI.

Chaffin, D.B., & Andersson, G.B.J. (1999). Occupational biomechanics. New York: John Wiley and Sons.

Chao, E.Y., Opgrande, J.D., & Axmear, F.E. (1976). Three-dimensional force analysis of finger joints in selected isometric hand functions. Journal of Biomechanics, 9, 387-396.

Crownishield, R. D. & Brand, R. A. (1981). A physiological based criterion of muscle force prediction in locomotion. Journal of Biomechanics, 14, 793-801.

Dysart, M.J. (1994). Development and validation of a posture prediction algorithm. Master's thesis, Virginia Polytechnic Institute and State University, Blacksburg, VA.

Faraway, J.J., & Hu, J. (2001). Modeling variability in reaching motions. SAE Technical Paper 2001-01-2094.

Granata, K.P., & Marras, W.S. (1996). Biomechanical models in ergonomics. Occupational ergonomics : Theory and applications / edited by Amit Bhattacharya, James D. McGlothlin. New York: Marcel Dekker.

Hirao, A., & Yamazaki, N. (1997). Synthesis of sitting posture by musculoskeletal model. Keio University, Japan: [http://tmc03.human.waseda.ac.jp/~wwdu97/PrcHP/130]

Hughes, R.E., Westreich, A., Rock, M.G., & An, K. (1997). Development of a three-dimensional arm strength prediction model. Proceedings of the American Society of Biomechanics 21th Annual Meeting, Clemson University, SC.

Jung, E.S., & Choe, J. (1996). Human reach posture prediction based on psychophysical discomfort. International Journal of Industrial Ergonomics, 18, 173-179.

Jung, E.S., & Kee, D. (1996). A man-machine interface model with improved visibility and reach functions. Computers Industrial Engineering, 30 (3), 475-486.

Jung, E.S., Kee, D., & Chung, M.K. (1992). Reach posture prediction of upper limb for ergonomic workspace evaluation. Proceedings of the Human Factors Society 36th Annual Meeting (pp 702-706). Santa Monica, CA: Human Factors Society.

Jung, E.S., Kee, D., & Chung, M.K. (1995). Upper body reach posture prediction for ergonomic evaluation models. International Journal of Industrial Ergonomics, 16, 95-107.

Jung, E.S., & Park, S. (1994). Prediction of human reach posture using a neural network for ergonomic man models. Computers Industrial Engineering, 27 (1-4), 369-372.

Kerk, C.J. (1992). Development and evaluation of a static hand force exertion capability model using strength, stability, and coefficient of friction. Doctoral dissertation, University of Michigan, Ann Arbor, MI.

Kilpatrick, K. (1970). A model for the design of manual workstations. Doctoral dissertation, University of Michigan, Ann Arbor, MI.

Landsmeer, J.M.F. (1963). The coordination of finger joint motions. Journal of Bone Joint Surg., 45, 1654-1662.

Lim, S. H., Jung, E. S., Chung, M. K. & Shin, Y. T. (1999). A two-segment trunk model for reach prediction. Proceedings of the International Cyberspace Conference on Ergonomics: CybErg 1999.

Marras, W.S., King, A.I., & Joynt, R.L. (1984). Measurements of loads on the lumbar spine under isometric and isokinetic conditions. Spine, 9, 176-188.

Marras, W.S., Lavender, S.A., Leurgans, S.E., Fathallah, F.A., Fersuson, S.A., Allread, W.G., & Rajulu, S.L. (1995). Biomechanical risk factors for occupationally-related low back disorders. Ergonomics, 28, 377-410.

Marras, W.S., & Schoenmarklin, R.W. (1990). A dynamic biomechanical model of the wrist joint. Proceedings of the Human Factors Society 34th Annual Meeting, Orlando, FL.

Marras, W.S., & Schoenmarklin, R.W. (1993). Wrist motions in industry. Ergonomics, 36, 341-351.

McMulkin, M.L. (1996). Investigation and empirical evaluation of inputs to optimization-based biomechanical trunk models. Doctoral dissertation, University of Michigan, Ann Arbor, MI.

Nussbaum, M.A., & Chaffin, D.B. (1996). Development and evaluation of a scalable and deformable geometric model of the human torso. Clinical Biomechanics, 11 (1), 25-34.

Nussbuam, M.A., Martin, B.J., & Chaffin, D.B. (1997). A neural network model for simulation of torso muscle coordination. Journal of Biomechanics, 30 (3), 251-258.

Pheasant, S. (1986). Bodyspace: Anthropometry, ergonomics and design. London: Taylor and Francis.

Ramsey, F.L., & Schafer, D.W. (1997). The statistical sleuth: A course in methods of data analysis. Belmont, CA: Wadsworth Publishing Company.

Roebuck, J.A., Kroemer, K., & Thomson, W.G. (1975). Engineering anthropometry methods. New York: Wiley-Interscience.

Shirazi-Adl, A. (1989). Stress in fibers of a lumbar disc, analysis of the role of lifting in producing disc prolapse. Spine, 14, 96-103.

Woldstad, J.C. (1996). A revised posture prediction algorithm for static lifting. Proceedings of First International Cyberspace Conference on Ergonomics.

APPENDICES

APPENDIX A: Force and Moment Calculations

A.1 Introduction to Calculation of Force and Moments

Forces and moments at each joint are calculated by using the theory of static mechanics that when the object (which is human, in this case) is static, the summation of forces and moments must be equal to zero. It can be written in terms of two balance equations of static forces and moments in free body diagram.

1. Balance of the forces

$$\Sigma F = 0 \tag{A.1}$$

Forces are investigated in two directions: horizontal (x-axis) and vertical (y-axis). Thus, the equation (3.1) can be expressed in this form:

$$\Sigma Fx = 0 \tag{A.2}$$

$$\Sigma Fy = 0 \tag{A.3}$$

2. Balances of the moments

$$\Sigma Mo = 0 \tag{A.4}$$

where,

F = force

Mo = moment applying at a joint due to external forces and link weight

All other variables that will be used to calculate forces and moments at each joint are described as follows:

Fx_i = the horizontal force at joint i due to external forces and link weight

Fy_i = the vertical force at joint i due to external forces and link weight

F_{XR} = the force from load applying to the right hand

F_{XL} = the force from load applying to the left hand

Mo_i = the total moment at joint i due to external forces and link weight.

C_i = the distance of the center of mass of link i relative to the orientation of joint i

L_i = the length of link i

The diagram of link i with moment and forces applied is shown in Figure A.1.

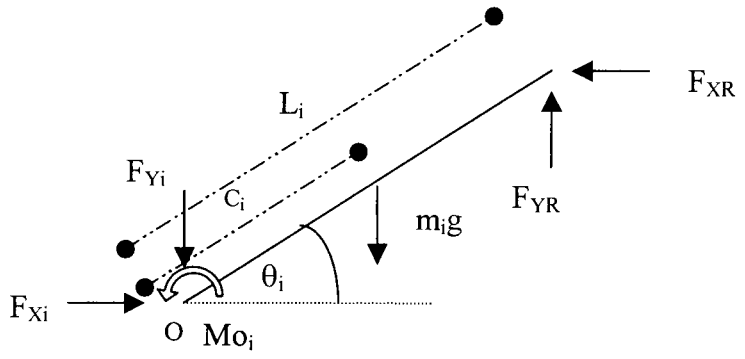

Figure A.1: Definition of link *i*.

A.2 Calculation of Moments and Forces at Each Joint

The calculations started at the hand joints where they deal with external force from the load and ended up at the feet on the floor. There is no moment at the hands because they are the positions that the external forces apply to. By using formulation described in the above section, forces and moments of each joint can be calculated and shown below.

1. Right Elbow (L_6)

Forces:

$$\Sigma F = 0 \tag{A.5}$$

Thus, the summation of forces in the x-direction must be equal to zero as well as in the y-direction.

From the free-body diagram shown in Figure, there are two forces in the x-direction. The equations can be written as follows:

$$\Sigma Fx = 0 \tag{A.6}$$

$$Fx_6 - F_{XR} = 0 \tag{A.7}$$

In order to find the value of Fx_6, equation (3.7) can be rewritten as:

$$Fx_6 = F_{XR} \tag{A.8}$$

On the other hand, there are three forces in the y-direction. The equations can also be expressed as follows:

$$\Sigma Fy = 0 \tag{A.9}$$

$$F_{YR} - Fy_6 - m_6 g = 0 \tag{A.10}$$

Thus,

$$Fy_6 = F_{YR} - m_6 g \tag{A.11}$$

Moments

From the free-body diagram shown in Figure A.2, the moment equations can be expressed as follows:

$$\Sigma Mo_{\text{right-elbow}} = 0 \tag{A.12}$$

$$Mo_6 - (m_6*g*C_6*L_6*\cos\theta_6) + (F_{XR}*L_6*\sin\theta_6) + (F_{YR}*L_6*\cos\theta_6) = 0 \quad (A.13)$$

$$Mo_6 = (m_6*g*C_6*L_6*\cos\theta_6) - (F_{XR}*L_6*\sin\theta_6) - (F_{YR}*L_6*\cos\theta_6) \quad (A.14)$$

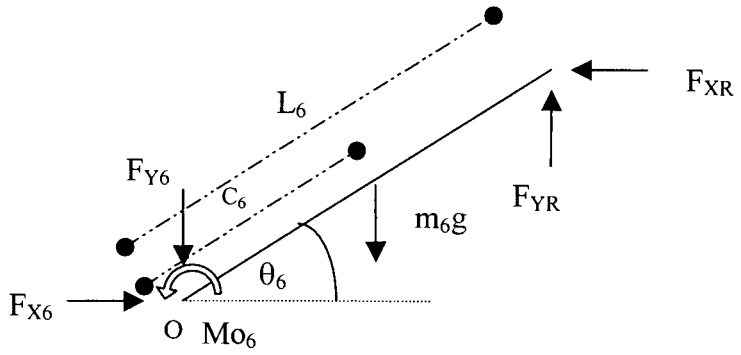

Figure A.2: Free body diagram of right elbow.

2. Left Elbow (L_7)

From Figure A.3, all the forces and moments equations can be described as follows:

Forces:

$$\Sigma F = 0 \quad (A.15)$$

$$\Sigma Fx = 0 \quad (A.16)$$

$$Fx_7 - F_{XL} = 0 \quad (A.17)$$

$$Fx_7 = F_{XL} \quad (A.18)$$

$$\Sigma Fy = 0 \tag{A.19}$$

$$F_{YL} - Fy_7 - (m_7 * g) = 0 \tag{A.20}$$

$$Fy_7 = F_{YL} - (m_7 * g) \tag{A.21}$$

Moments:

$$\Sigma Mo_{left\text{-}elbow} = 0 \tag{A.22}$$

$$Mo_7 - (m_7 * g * C_7 * L_7 * \cos\theta_7) + (F_{XL} * l_7 * \sin\theta_7) + (F_{YL} * l_7 * \cos\theta_7) = 0 \tag{A.23}$$

$$Mo_7 = (m_7 * g * C_7 * L_7 * \cos\theta_7) - (F_{XL} * l_7 * \sin\theta_7) - (F_{YL} * l_7 * \cos\theta_7) \tag{A.24}$$

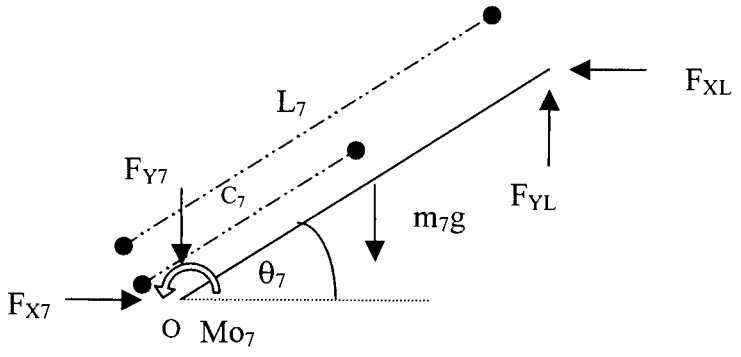

Figure A.3: Free body diagram of left elbow.

3. Right Shoulder (L_9)

From Figure A.4, all the forces and moments equations can be described as follows:

Forces:

$$\Sigma F = 0 \tag{A.25}$$

$$\Sigma Fx = 0 \tag{A.26}$$

$$Fx_9 - Fx_6 = 0 \tag{A.27}$$

$$Fx_9 = Fx_6 = F_{XR} \tag{A.28}$$

$$\Sigma Fy = 0 \tag{A.29}$$

$$Fy_6 - Fy_9 - (m_9 * g) = 0 \tag{A.30}$$

$$Fy_9 = Fy_6 - (m_9 * g) \tag{A.31}$$

$$Fy_9 = F_{YR} - (m_6 * g) - (m_9 * g) \tag{A.32}$$

Moments:

$$\Sigma Mo_{\text{right-shoulder}} = 0 \tag{A.33}$$

$$Mo_9 - Mo_6 - (m_9 * g * C_9 * L_9 * \cos\theta_9) + (Fx_6 * L_9 * \sin\theta_9) + (Fy_6 * L_9 * \cos\theta_9) \tag{A.34}$$

$$Mo_9 = Mo_6 + (m_9 * g * C_9 * L_9 * \cos\theta_9) - (Fx_6 * l_9 * \sin\theta_9) - (Fy_6 * L_9 * \cos\theta_9) \tag{A.35}$$

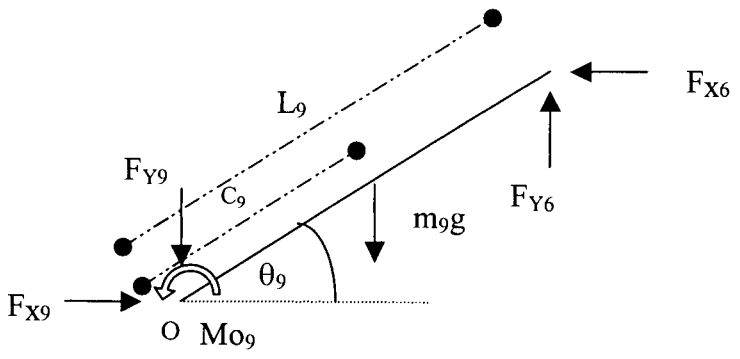

Figure A.4: Free body diagram of right shoulder.

4. Left Shoulder (L_8)

From Figure A.5, all the forces and moments equations can be described as follows:

Forces:

$$\Sigma F = 0 \tag{A.36}$$

$$\Sigma Fx = 0 \tag{A.37}$$

$$Fx_8 - Fx_7 = 0 \tag{A.38}$$

$$Fx_8 = Fx_7 = F_{XL} \tag{A.39}$$

$$\Sigma Fy = 0 \tag{A.40}$$

$$Fy_7 - Fy_8 - (m_8 * g) = 0 \tag{A.41}$$

$$Fy_8 = Fy_7 - (m_8 * g) = F_{YL} - (m_7 * g) - (m_8 * g) \tag{A.42}$$

Moments:

$$\Sigma Mo_{\text{left-shoulder}} = 0 \tag{A.43}$$

$$Mo_8 - Mo_7 - (m_8 * g * C_8 * l_8 * \cos\theta_8) + (Fx_7 * l_8 * \sin\theta_8) + (Fy_7 * L_8 * \cos\theta_8) \tag{A.44}$$

$$Mo_8 = Mo_7 + (m_8 * g * C_8 * l_8 * \cos\theta_8) - (Fx_7 * l_8 * \sin\theta_8) - (Fy_7 * L_8 * \cos\theta_8) \tag{A.45}$$

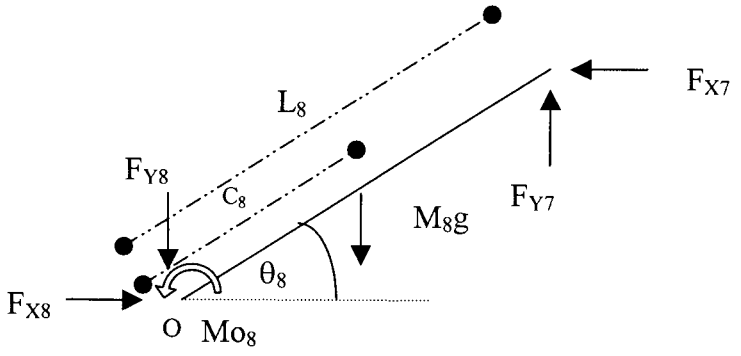

Figure A.5: Free body diagram of left shoulder.

5. Neck (L_{10})

From Figure A.6, all the forces and moments equations can be described as follows:

Forces:

$$\Sigma F = 0 \qquad \text{(A.46)}$$

Since there is no force applied to the neck except from its weight, thus,

$$\Sigma Fx = 0 \qquad \text{(A.47)}$$

$$Fx_{10} = 0 \qquad \text{(A.48)}$$

$$\Sigma Fy = 0 \qquad \text{(A.49)}$$

$$-Fy_{10} - (m_{10}*g) = 0 \qquad \text{(A.50)}$$

$$Fy_{10} = -(m_{10}*g) \qquad \text{(A.51)}$$

Moments:

$$\Sigma Mo_{neck} = 0 \quad \text{(A.52)}$$

$$Mo_{10} - (m_{10}*g*C_{10}*L_{10}*\cos\theta_{10}) = 0 \quad \text{(A.53)}$$

$$Mo_{10} = (m_{10}*g*C_{10}*L_{10}*\cos\theta_{10}) \quad \text{(A.54)}$$

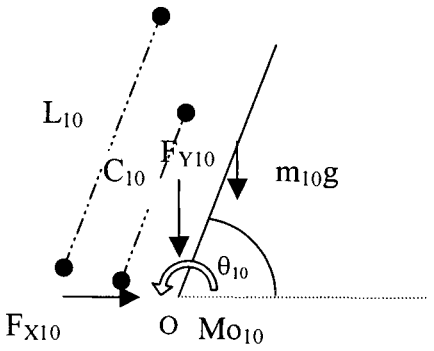

Figure A.6: Free body diagram of neck.

6. Hip (L_5)

From Figure A.7, all forces and moments equations can be described as follows:

Forces:

$$\Sigma F = 0 \quad \text{(A.55)}$$

$$\Sigma Fx = 0 \quad \text{(A.56)}$$

$$Fx_5 - Fx_8 - Fx_9 - Fx_{10} = 0 \quad \text{(A.57)}$$

$$Fx_5 = Fx_8 + Fx_9 + Fx_{10} = F_{XL} + F_{XR} \quad \text{(A.58)}$$

$$\Sigma Fy = 0 \tag{A.59}$$

$$Fy_8 + Fy_9 + Fy10 - Fy_5 - (m_5 * g) = 0 \tag{A.60}$$

$$Fy_5 = Fy_8 + Fy_9 + Fy_{10} - (m_5 * g) \tag{A.61}$$

$$Fy_5 = F_{YL} + F_{YR} + Fy_{10} - ((m_5 + m_6 + m_7 + m_8 + m_9 + m_{10}) * g) \tag{A.62}$$

Moments:

$$\Sigma Mo_{hip} = 0 \tag{A.63}$$

$$Mo_5 - (Mo_8 + Mo_9 + Mo_{10}) + (Fx_8 + Fx_9 + Fx_{10}) * L_5 * \sin\theta_5 \tag{A.64}$$

$$+ (Fy_8 + Fy_9 + Fy_{10}) * L_5 * \cos\theta_5 - (m_5 * g * C_5 * L_5 * \cos\theta_5) = 0$$

$$Mo_5 = (Mo_8 + Mo_9 + Mo_{10}) - (Fx_8 + Fx_9 + Fx_{10}) * L_5 * \sin\theta_5 \tag{A.65}$$

$$- (Fy_8 + Fy_9 + Fy_{10}) * L_5 * \cos\theta_5 + (m_5 * g * C_5 * L_5 * \cos\theta_5)$$

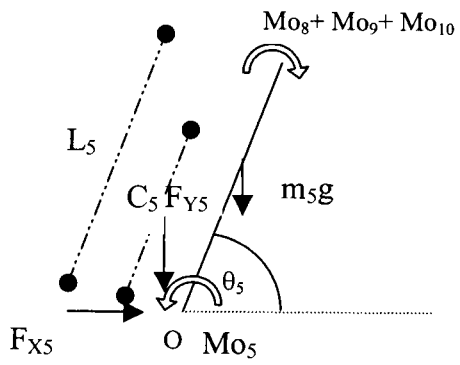

Figure A.7: Free body diagram of hip.

7. Right Knee (L_4)

From Figure A.8, all forces and moments equations can be described as follows:

Forces:

$$\Sigma F = 0 \tag{A.66}$$

$$\Sigma Fx = 0 \tag{A.67}$$

$$Fx_4 - (Fx_5)/2 = 0 \tag{A.68}$$

$$Fx_4 = (Fx_5)/2 = (1/2)(F_{XL} + F_{XR}) \tag{A.69}$$

$$\Sigma Fy = 0 \tag{A.70}$$

$$(Fy_5)/2 - Fy_4 - (m_4*g) = 0 \tag{A.71}$$

$$Fy_4 = (Fy_5)/2 - (m_4*g) \tag{A.72}$$

$$Fy_4 = (1/2)(F_{YL} + F_{YR} - (m_5 + m_6 + m_7 + m_8 + m_9 + m_{10})*g) - (m_4*g) \tag{A.73}$$

Moments:

$$\Sigma Mo_{right\text{-}knee} = 0 \tag{A.74}$$

$$Mo_4 - (Mo_5/2) + (Fx_5/2)*L_4*\sin(180 - \theta_4) - (Fy_5/2)*L_4*\cos(180 - \theta_4) + (m_4*g*C_4*L_4*\cos(180\text{-}\theta_4)) = 0 \tag{A.75}$$

$$Mo_4 = (Mo_5/2) - (Fx_5/2)*L_4*\sin(180\text{–}\theta_4) + (Fy_5/2)*L_4*\cos(180 - \theta_4) - (m_4*g*C_4*l_4*\cos(180 - \theta_4)) \tag{A.76}$$

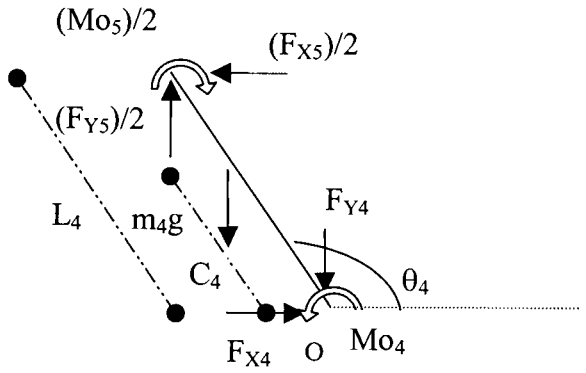

Figure A.8: Free body diagram of right knee.

8. Left Knee (L_3)

From Figure A.9, all forces and moments equations can be described as follows:

Forces:

$$\Sigma F = 0 \qquad \text{(A.77)}$$

$$\Sigma Fx = 0 \qquad \text{(A.78)}$$

$$Fx_3 - (Fx_5)/2 = 0 \qquad \text{(A.79)}$$

$$Fx_3 = (Fx_5)/2 = (1/2)(F_{XL} + F_{XR}) \qquad \text{(A.80)}$$

$$\Sigma Fy = 0 \qquad \text{(A.81)}$$

$$(Fy_5)/2 - Fy_3 - (m_3 * g) = 0 \qquad \text{(A.82)}$$

$$Fy_3 = (Fy_5)/2 - (m_3 * g) \qquad \text{(A.83)}$$

$$Fy_3 = (1/2)(F_{YL} + F_{YR} - (m_5 + m_6 + m_7 + m_8 + m_9 + m_{10}) * g) - (m_3 * g) \qquad \text{(A.84)}$$

Moments:

$$\Sigma Mo_{left\text{-}knee} = 0 \tag{A.85}$$

$$Mo_3 - (Mo_5/2) + (Fx_5/2)*L_3*\sin(\theta_3) \tag{A.86}$$
$$+ (Fy_5/2)*L_3*\cos(\theta_3) - m_3*g*C_3*L_3*\cos(\theta_3) = 0$$

$$Mo_3 = (Mo_5/2) - (Fx_5/2)*L_3*\sin(\theta_3) \tag{A.87}$$
$$- (Fy_5/2)*L_3*\cos(\theta_3) + m_3*g*C_3*L_3*\cos(\theta_3)$$

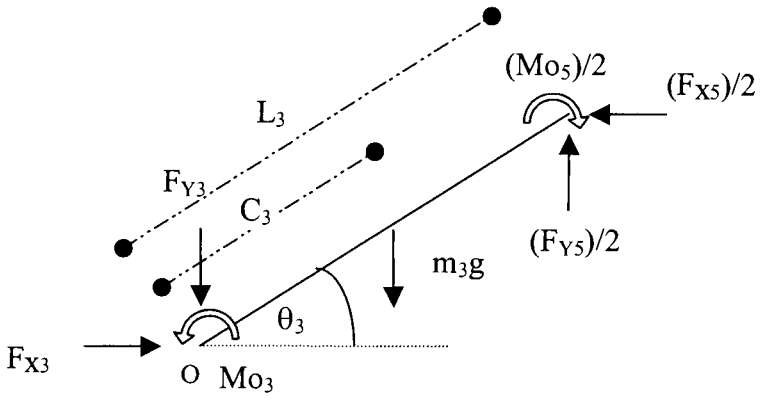

Figure A.9: Free body diagram of left knee.

9. Right Ankle (L_1)

From Figure A.10, all forces and moments equations can be described as follows:

Forces:

$$\Sigma F = 0 \tag{A.88}$$

$$\Sigma Fx = 0 \tag{A.99}$$

$$Fx_1 - Fx_4 = 0 \tag{A.100}$$

$$Fx_1 = Fx_4 = (1/2)(F_{XL} + F_{XR}) \tag{A.101}$$

$$\Sigma Fy = 0 \tag{A.102}$$

$$Fy_4 - Fy_1 - (m_1 * g) = 0 \tag{A.103}$$

$$Fy_1 = Fy_4 - (m_1 * g) \tag{A.104}$$

$$Fy_1 = (1/2)(F_{YL} + F_{YR} - (m_5 + m_6 + m_7 + m_8 + m_9 + m_{10}) * g) - (m_4 * g) - (m_1 * g) \tag{A.105}$$

Moments:

$\Sigma M_{right\text{-}ankle} = 0$

$$Mo_1 - Mo_4 + Fx_4 * L_1 * \sin(180 - \theta_1) - Fy_4 * L_1 * \cos(180 - \theta_1) + m_1 * g * C_1 * L_1 * \cos(180 - \theta_1) = 0 \tag{A.106}$$

$$Mo_1 = Mo_4 - Fx_4 * L_1 * \sin(180 - \theta_1) + Fy_4 * L_1 * \cos(180 - \theta_1) - m_1 * g * C_1 * L_1 * \cos(180 - \theta_1) \tag{A.107}$$

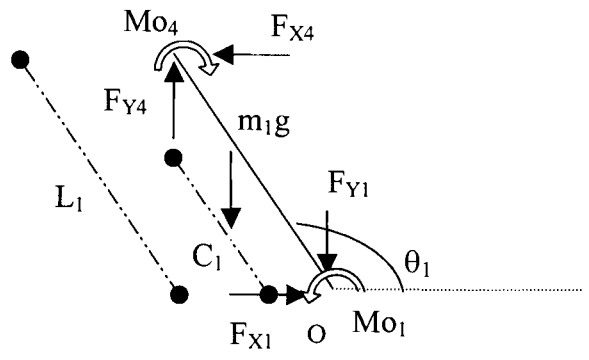

Figure A.10: Free body diagram of right ankle.

10. Left Ankle (L_2)

From Figure A.11, all forces and moments equations can be described as follows:

Forces:

$$\Sigma F = 0 \qquad \text{(A.108)}$$

$$\Sigma Fx = 0 \qquad \text{(A.109)}$$

$$Fx_2 - Fx_3 = 0 \qquad \text{(A.110)}$$

$$Fx_2 = Fx_3 = (Fx_5)/2 = (1/2)(F_{XL} + F_{XR}) \qquad \text{(A.111)}$$

$$\Sigma Fy = 0 \qquad \text{(A.112)}$$

$$Fy_3 - Fy_2 - (m_2 * g) = 0 \qquad \text{(A.113)}$$

$$Fy_2 = Fy_3 - (m_2 * g) \qquad \text{(A.114)}$$

$$Fy_2 = (1/2)(F_{YL} + F_{YR} - (m_5 + m_6 + m_7 + m_8 + m_9 + m_{10})*g) \quad (A.115)$$

$$- (m_3*g) - (m_2*g)$$

Moments:

$$\Sigma M_{left\text{-}ankle} = 0 \quad (A.116)$$

$$Mo_2 - Mo_3 + Fx_3*L_2*\sin(\theta_2) + Fy_3*L_2*\cos(\theta_2) - m_2*g*C_2*L_2*\cos(\theta_2) = 0 \quad (A.117)$$

$$Mo_2 = Mo_3 - Fx_3*L_2*\sin(\theta_2) - Fy_3*L_2*\cos(\theta_2) + m_2*g*C_2*L_2*\cos(\theta_2) \quad (A.118)$$

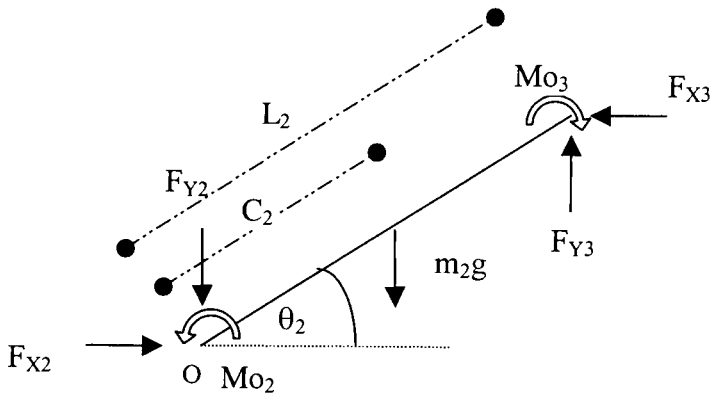

Figure A.11: Free body diagram of left ankle.

A.2 Calculation of Moments and Forces at the Heel and Ball of the Feet

A.2.1 Right Foot

From Figure A.12, all forces and moments equations can be described as follows:

Forces:

$$\Sigma F = 0 \tag{A.119}$$

$$\Sigma Fx = 0 \tag{A.120}$$

$$Fx_{br} - Fx_l = 0 \tag{A.121}$$

$$Fx_{br} = Fx_l \tag{A.122}$$

$$\Sigma Fy = 0 \tag{A.123}$$

$$Fy_{br} - Fy_l + (m_f * g) = 0 \tag{A.124}$$

$$Fy_{br} = Fy_l - (m_f * g) \tag{A.125}$$

Moments:

$$\Sigma M_{ball\text{-}right} = 0 \tag{A.126}$$

$$-Mo_l + Mo_{br} + m_f * g * l_4 + Fx_l * l_6 - F_{Yl} * (l_3 + l_4) = 0 \tag{A.127}$$

$$Mo_{br} = Mo_l - m_f * g * l_4 - Fx_l * l_6 + F_{Yl} * (l_3 + l_4) \tag{A.128}$$

$$\Sigma M_{heel\text{-}right} = 0 \tag{A.129}$$

$$-Mo_l + Mo_{hr} - m_f * g * (l_l + l_2 + l_3) + Fx_l * l_6 + F_{Yl} * (l_l + l_2) = 0 \tag{A.130}$$

$$Mo_{hr} = Mo_l + m_f * g * (l_l + l_2 + l_3) - Fx_l * l_6 - F_{Yl} * (l_l + l_2) \tag{A.131}$$

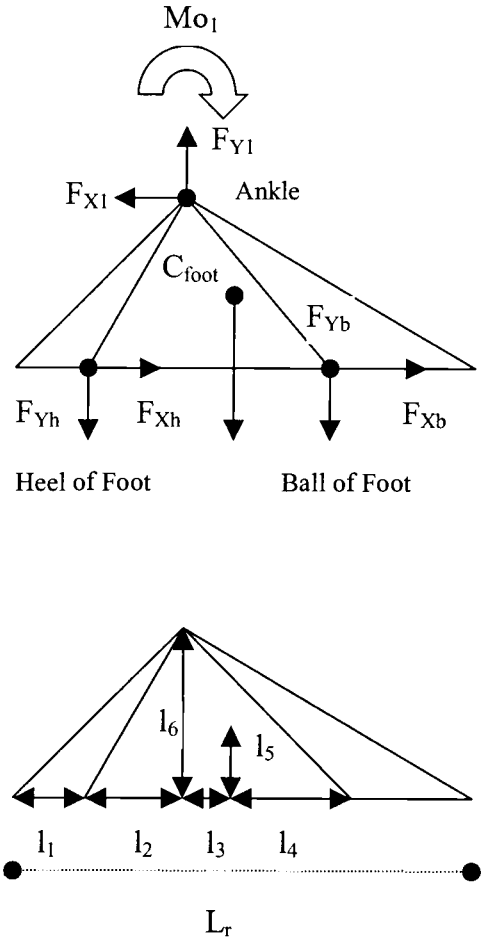

Figure A.12: Free body diagram of right foot.

A.2.2 Left Foot

From Figure A.13, all forces and moments equations can be described as follows:

Forces:

$$\Sigma F = 0 \tag{A.132}$$

$$\Sigma Fx = 0 \tag{A.133}$$

$$Fx_{bl} - Fx_2 = 0 \tag{A.134}$$

$$Fx_{bl} = Fx_2 \tag{A.135}$$

$$\Sigma Fy = 0 \tag{A.136}$$

$$Fy_{bl} - Fy_2 + (m_f * g) = 0 \tag{A.137}$$

$$Fy_{bl} = Fy_2 - (m_f * g) \tag{A.138}$$

Moments:

$$\Sigma M_{ball\text{-}left} = 0 \tag{A.139}$$

$$-Mo_2 + Mo_{bl} + m_f * g * l_4 + Fx_2 * l_6 - F_{Y2} * (l_3 + l_4) = 0 \tag{A.140}$$

$$Mo_{bl} = Mo_2 - m_f * g * l_4 - Fx_2 * l_6 + F_{Y2} * (l_3 + l_4) \tag{A.141}$$

$$\Sigma M_{heel\text{-}left} = 0 \tag{A.142}$$

$$-Mo_2 + Mo_{hl} - m_f * g * (l_1 + l_2 + l_3) + Fx_2 * l_6 + F_{Y2} * (l_1 + l_2) = 0 \tag{A.143}$$

$$Mo_{hl} = Mo_2 + m_f * g * (l_1 + l_2 + l_3) - Fx_2 * l_6 - F_{Y2} * (l_1 + l_2) \tag{A.144}$$

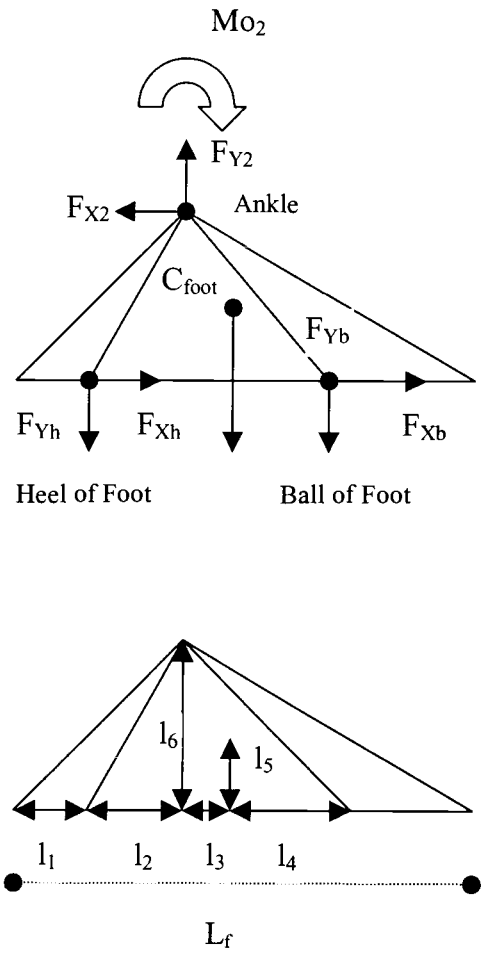

Figure A.13: Free body diagram of left foot.

APPENDIX B: Posture Prediction Model

Posture Prediction Model

Minimize $(Mo_1)^2 + (Mo_2)^2 + (Mo_3)^2 + (Mo_4)^2 + (Mo_5)^2 + (Mo_6)^2 + (Mo_7)^2 + (Mo_8)^2 + (Mo_9)^2 + (Mo_{10})^2 + (Mo_{br} + Mo_{hr} + Mo_{bl} + Mo_{hl})^2$

$Mo_1 = Mo_4 - (F_{X4}*L_1*\sin(180-(\theta_1))) + (F_{Y4}*L_1*\cos(180-(\theta_1))) - (m_1*g*0.629*L_1*\cos(180-(\theta_1)))$

$Mo_2 = Mo_3 - (F_{X3}*L_2*\sin(\theta_2)) - (F_{Y3}*L_2*\cos(\theta_2)) + (m_2*g*0.629*L_2*\cos(\theta_2))$

$Mo_3 = (Mo_5/2) - ((F_{X5}/2)*L_3*\sin(\theta_3)) - ((F_{Y5}/2)*L_3*\cos(\theta_3)) + (m_3*g*0.628*L_3*\cos(\theta_3))$

$Mo_4 = (Mo_5/2) - ((F_{X5}/2)*L_4*\sin(180-(\theta_4))) + ((F_{Y5}/2)*L_4*\cos(180-(\theta_4))) - (m_4*g*0.628*L_4*\cos(180-(\theta_4)))$

$Mo_5 = Mo_8 + Mo_9 + Mo_{10} - ((F_{X8} + F_{X9} + F_{X10})*L_5*\sin(\theta_5)) - ((F_{Y8} + F_{Y9} + F_{Y10})*L_5*\cos(\theta_5)) + (m_5*g*0.38*L_5*\cos(\theta_5))$

$Mo_6 = -(F_{XR}*L_6*\sin(\theta_6)) - (F_{YR}*L_6*\cos(\theta_6)) + (m_6*g*0.39*L_6*\cos(\theta_6))$

$Mo_7 = -(F_{XL}*L_7*\sin(\theta_7)) - (F_{YL}*L_7*\cos(\theta_7)) + (m_7*g*0.39*L_7*\cos(\theta_7))$

$Mo_8 = Mo_7 - (F_{X7}*L_8*\sin(\theta_8)) - (F_{Y7}*L_8*\cos(\theta_8)) + (m_8*g*(1-0.513)*L_8*\cos(\theta_8))$

$Mo_9 = Mo_6 - (F_{X6}*L_9*\sin(\theta_9)) - (F_{Y6}*L_9*\cos(\theta_9)) + (m_9*g*(1-0.513)*L_9*\cos(\theta_9))$

$Mo_{10} = m_{10}*g*0.466*L_{10}*\cos(\theta_{10})$

$Mo_{hr} = Mo_1 - (F_{X1}*0.264*L_f) - (F_{Y1}*0.083*L_f) + (m_f*g*0.315*L_f)$

$Mo_{br} = Mo_1 - (F_{X1}*0.264*L_f) + (F_{Y1}*0.662*L_f) - (m_f*g*0.43*L_f)$

$Mo_{hl} = Mo_2 - (F_{X2}*0.264*L_f) - (F_{Y2}*0.083*L_f) + (m_f*g*0.315*L_f)$

$Mo_{bl} = Mo_2 - (F_{X2}*0.264*L_f) + (F_{Y2}*0.662*L_f) - (m_f*g*0.43*L_f)$

Forces:

$F_{X1} = (1/2)*(F_{XL} + F_{XR})$

$F_{Y1} = ((1/2)*(F_{YL} + F_{YR} - ((m_5 + m_6 + m_7 + m_8 + m_9 + m_{10})*g))) - (m_4*g) - (m_1*g)$

$F_{X2} = (1/2)*(F_{XL} + F_{XR})$

$F_{Y2} = ((1/2)*(F_{YL} + F_{YR} - ((m_5 + m_6 + m_7 + m_8 + m_9 + m_{10})*g))) - (m_3*g) - (m_2*g)$

$F_{X3} = (1/2)*(F_{XL}+F_{XR})$

$F_{Y3} = ((1/2)*(F_{YL} + F_{YR} - ((m_5 + m_6 + m_7 + m_8 + m_9 + m_{10})*g))) - (m_3*g)$

$F_{X4} = (1/2)*(F_{XL} + F_{XR})$

$F_{Y4} = ((1/2)*(F_{YL} + F_{YR} - ((m_5 + m_6 + m_7 + m_8 + m_9 + m_{10})*g))) - (m_4*g)$

$F_{X5} = F_{XL} + F_{XR}$

$F_{Y5} = F_{YL} + F_{YR} - ((m_5 + m_6 + m_7 + m_8 + m_9 + m_{10})*g)$

$F_{X6} = F_{XR}$

$F_{Y6} = F_{YR} - (m_6*g)$

$F_{X7} = F_{XL}$

$F_{Y7} = F_{YL} - (m_7*g)$

$F_{X8} = F_{XL}$

$F_{Y8} = F_{YR} - (m_7*g) - (m_8*g)$

$F_{X9} = F_{XR}$

$F_{Y9} = F_{YR} - (m_6*g) - (m_9*g)$

$F_{X10} = 0$

$F_{Y10} = -m_{10}*g$

Subject to

Constraints related to hands:

Left Hand

$X_L = L_1*\cos(\theta_1) + L_4*\cos(\theta_4) + L_5*\cos(\theta_5) + L_7*\cos(\theta_7) + L_8*\cos(\theta_8)$

$Y_L = L_1*\sin(\theta_1) + L_4*\sin(\theta_4) + L_5*\sin(\theta_5) + L_7*\sin(\theta_7) + L_8*\sin(\theta_8) + (0.264*L_f)$

Right Hand

$X_R = L_1*\cos(\theta_1) + L_4*\cos(\theta_4) + L_5*\cos(\theta_5) + L_6*\cos(\theta_6) + L_9*\cos(\theta_9)$

$Y_R = L_1*\sin(\theta_1) + L_4*\sin(\theta_4) + L_5*\sin(\theta_5) + L_6*\sin(\theta_6) + L_9*\sin(\theta_9) + (0.264*L_f)$

Line of Sight

$X_S = -(L_6*\cos(\theta_6)+L_9*\cos(\theta_9))$

$Y_S = L_1*\sin(\theta_1) + L_4*\sin(\theta_4) + L_5*\sin(\theta_5) + (0.264*L_f)$

$X_N = -(L_6*\cos(\theta_6) + L_9*\cos(\theta_9) - L_{10}*\cos(\theta_{10\text{-}P}))$

$Y_N = L_1*\sin(\theta_1) + L_4*\sin(\theta_4) + L_5*\sin(\theta_5) + L_{10}*\sin(\theta_{10\text{-}P}) + (0.264*L_f)$

$X = (X_L+X_R)/2$

$Y = (Y_L+Y_R)/2$

$A = (X_N-X_S)^2 + (Y_N-Y_S)^2$

$B = (X-X_N)^2 + (Y-Y_N)^2$

$C = (X-X_S)^2 + (Y-Y_S)^2$

$C = A + B$

$X > X_S$

$X > X_N$

$\theta_{10} \geq \theta_{10\text{-}P} - (10*Pi/180)$

$\theta_{10} \leq \theta_{10\text{-}P} + (24*Pi/180)$

Constraints related to human body:

Range of Motion (in radians)

Pi = 3.14159265359;

$29*Pi/180$	$\leq$	θ_1	$\leq$	$153*Pi/180$	(Right Ankle)
$29*Pi/180$	$\leq$	θ_2	$\leq$	$153*Pi/180$	(Left Ankle)
$0*Pi/180$	$\leq$	$\theta_3-\theta_2$	$\leq$	$174*Pi/180$	(Left Knee)
$0*Pi/180$	$\leq$	$\theta_4-\theta_1$	$\leq$	$174*Pi/180$	(Right Knee)
$-180*Pi/180$	$\leq$	$\theta_5-\theta_4$	$\leq$	$50*Pi/180$	(Right Thigh-Hip)
$-180*Pi/180$	$\leq$	$\theta_5-\theta_3$	$\leq$	$50*Pi/180$	(Left Thigh-Hip)
$-240*Pi/180$	$\leq$	$\theta_8-\theta_5$	$\leq$	$10*Pi/180$	(Hip-Left Shoulder)
$-240*Pi/180$	$\leq$	$\theta_9-\theta_5$	$\leq$	$10*Pi/180$	(Hip-Right Shoulder)
0	$\leq$	$\theta_6-\theta_9$	$\leq$	$180*Pi/180$	(Right Elbow)
0	$\leq$	$\theta_7-\theta_8$	$\leq$	$180*Pi/180$	(Left Elbow)
$-70*Pi/180$	$\leq$	$\theta_{10}-\theta_5$	$\leq$	$20*Pi/180$	(Neck-Torso)

$|\theta_4 - \theta_3| \leq 135*Pi/180$ (Distance between both legs)

Constraint related to the feet (both feet must be on floor):

$L_2*\sin(\theta_2) + L_3*\sin(\theta_3) = L_1*\sin(\theta_1) + L_4*\sin(\theta_4)$

Constraint related to the shoulders:

$L_6*\cos(\theta_6) + L_9*\cos(\theta_9) = L_7*\cos(\theta_7) + L_8*\cos(\theta_8) - X_L$

Constraints related to balance:

$X_{hr} = -((L_6*\cos(\theta_6)) + (L_9*\cos(\theta_9)) + (L_5*\cos(\theta_5)) + (L_1*\cos(\theta_1)) + (L_4*\cos(\theta_4)) + (0.083*L_f))$

$X_{hl} = -((L_6*\cos(\theta_6)) + (L_9*\cos(\theta_9)) + (L_5*\cos(\theta_5)) + (L_2*\cos(\theta_2)) + (L_3*\cos(\theta_3)) +(0.083*L_f))$

$X_{br} = -((L_6*\cos(\theta_6)) + (L_9*\cos(\theta_9)) + (L_5*\cos(\theta_5)) + (L_1*\cos(\theta_1)) + (L_4*\cos(\theta_4))-(0.662*L_f))$

$X_{bl} = -((L_6*\cos(\theta_6)) + (L_9*\cos(\theta_9)) + (L_5*\cos(\theta_5)) + (L_2*\cos(\theta_2)) + (L_3*\cos(\theta_3))-(0.662*L_f))$

$X_{heel} = \text{Minimum}(X_{hl}, X_{hr})$

$X_{ball} = \text{Maximum}(X_{bl}, X_{br})$

$X_1 = -(L_6*\cos(\theta_6)) - (L_9*\cos(\theta_9)) - (L_5*\cos(\theta_5)) - (L_4*\cos(\theta_4)) -(0.371* L_1*\cos(\theta_1))$

$X_2 = -(L_6*\cos(\theta_6)) - (L_9*\cos(\theta_9)) - (L_5*\cos(\theta_5)) - (L_3*\cos(\theta_3)) -(0.371* L_2*\cos(\theta_2))$

$$X_3 = -(L_6*\cos(\theta_6)) - (L_9*\cos(\theta_9)) - (L_5*\cos(\theta_5)) - (0.372*L_3*\cos(\theta_3))$$

$$X_4 = -(L_6*\cos(\theta_6)) - (L_9*\cos(\theta_9)) - (L_5*\cos(\theta_5)) - (0.372*L_4*\cos(\theta_4))$$

$$X_5 = -(L_6*\cos(\theta_6)) - (L_9*\cos(\theta_9)) - 0.62*(L_5*\cos(\theta_5))$$

$$X_6 = -0.61*(L_6*\cos(\theta_6))$$

$$X_7 = -0.61*(L_7*\cos(\theta_7)) + X_L$$

$$X_8 = (-(L_7*\cos(\theta_7))) - (0.513*L_8*\cos(\theta_8)) + X_L$$

$$X_9 = (-(L_6*\cos(\theta_6))) - (0.513*L_9*\cos(\theta_9))$$

$$X_{10} = (-(L_6*\cos(\theta_6))) - (L_9*\cos(\theta_9)) + (0.466*L_{10}*\cos(\theta_{10}))$$

$$X_{fr} = (-(L_6*\cos(\theta_6))) - (L_9*\cos(\theta_9)) - (L_5*\cos(\theta_5)) - (L_4*\cos(\theta_4))$$
$$-(L_1*\cos(\theta_1)) + ((0.44-0.208)*L_f)$$

$$X_{fl} = (-(L_6*\cos(\theta_6))) - (L_9*\cos(\theta_9)) - (L_5*\cos(\theta_5)) - (L_3*\cos(\theta_3))$$
$$-(L_2*\cos(\theta_2)) + ((0.44-0.208)*L_f)$$

Stability Constraints:

Prevent from tipping backward

$$((F_{xr}*Y_R) + (F_{xl}*Y_L) - (F_{yr}*X_{heel}) - (F_{yl}*(X_L-X_{heel}))) \leq$$
$$9.81*((m_1*(X_1-X_{heel})) + (m_2*(X_2-X_{heel})) + (m_3*(X_3-X_{heel})) + (m_4*(X_4-X_{heel})) +$$
$$(m_5*(X_5-X_{heel})) + (m_6*(X_6-X_{heel})) + (m_7*(X_7-X_{heel})) + (m_8*(X_8-Xheel)) + (m_9*(X_9-$$
$$X_{heel})) + (m_{10}*(X_{10}-X_{heel})) + (m_f*(X_{fr}-X_{heel})) + (m_f*(X_{fr}-X_{heel})))$$

Prevent from tipping forward

$$((F_{xr}*Y_R) + (F_{xl}*Y_L) - (F_{yr}*X_{ball}) - (F_{yl}*(X_L-X_{ball}))) \geq$$

$$9.81*((m_1*(X_1-X_{ball})) + (m_2*(X_2-X_{ball})) + (m_3*(X_3-X_{ball})) + (m_4*(X_4-X_{ball})) + (m_5*(X_5-X_{ball})) + (m_6*(X_6-X_{ball})) + (m_7*(X_7-X_{ball})) + (m_8*(X_8-Xball)) + (m_9*(X_9-X_{ball})) + (m_{10}*(X_{10}-X_{ball})) + (m_f*(X_{fr}-X_{ball})) + (m_f*(X_{fr}-X_{ball})))$$

APPENDIX C: Posture Prediction Lingo Code

```
!(POSTURE PREDICTION MODEL);
!(BY THIDARAT DENDAMRONGVIT, OREGON STATE UNIVERSITY);

MODEL:

!INPUT;

!HAND LOAD;

!HAND POSITION;

DATA:

!IMPORT DATA FROM THE EXCEL FILE;

!LEFT AND RIGHT HAND LOADS;

Fxl = @OLE( 'C:\My Documents\posture--righthand.XLS');
Fxr = @OLE( 'C:\My Documents\posture--righthand.XLS');
Fyl = @OLE( 'C:\My Documents\posture--righthand.XLS');
Fyr = @OLE( 'C:\My Documents\posture--righthand.XLS');

!LEFT HAND AND RIGHT HAND POSITIONS;
!Xr MUST BE ZERO;

Xl = @OLE( 'C:\My Documents\posture--righthand.XLS');
Xr = @OLE( 'C:\My Documents\posture--righthand.XLS');
Yl = @OLE( 'C:\My Documents\posture--righthand.XLS');
Yr = @OLE( 'C:\My Documents\posture--righthand.XLS');

ENDDATA

!END IMPORT DATA FROM THE EXCEL FILE;

!ALLOWING IT TO TAKE ANY POSITIVE OR NEGATIVE VALUE;

@FREE(Fxl);
@FREE(Fxr);
@FREE(Fyl);
@FREE(Fyr);
@FREE(Xl);

!OBJECTIVE FUNCTION;

!SUM OF MOMENT SQUARES;

MIN =
(MO1)^2+(MO2)^2+(MO3)^2+(MO4)^2+(MO5)^2+(MO6)^2+(MO7)^2+(MO8)^2
+(MO9)^2+(MO0)^2+(MObr+MOhr+MObl+MOhl)^2;
```

```
!MOMENT CALCULATIONS;

MO1 = MO4-((Fx4)*(L1)*@SIN(180-(Q1)))+((Fy4)*(L1)*@COS(180-(Q1)))-
((m1)*g*0.629*(L1)*@COS (180-(Q1)));

MO2 = MO3-((Fx3)*(L2)*@SIN(Q2))-
((Fy3)*(L2)*@COS(Q2))+((m2)*g*0.629*(L2)*@COS(Q2));

MO3 = (MO5/2)-((Fx5)/2*(L3)*@SIN(Q3))-
((Fy5)/2*(L3)*@COS(Q3))+((m3)*g*0.628*(L3)*@COS (Q3));

MO4 = (MO5/2)-((Fx5)/2*(L4)*@SIN(180-(Q4)))+((Fy5)/2*(L4)*@COS(180-
(Q4)))-((m4)*g*0.628*    (L4)*@COS(180-(Q4)));

MO5 = MO8+MO9+MO0-((Fx8+Fx9+Fx0)*(L5)*@SIN(Q5))-
((Fy8+Fy9+Fy0)*(L5)*@COS(Q5))+((m5)*g*     0.38*(L5)*@COS(Q5));

MO6 = -((Fxr)*(L6)*@SIN(Q6))-
((Fyr)*(L6)*@COS(Q6))+((m6)*g*0.39*(L6)*@COS(Q6));

MO7 = -((Fxl)*(L7)*@SIN(Q7))-
((Fyl)*(L7)*@COS(Q7))+((m7)*g*0.39*(L7)*@COS(Q7));

MO8 = MO7-((Fx7)*(L8)*@SIN(Q8))-((Fy7)*(L8)*@COS(Q8))+((m8)*g*(1-
0.513)*(L8)*@COS(Q8));

MO9 = MO6-((Fx6)*(L9)*@SIN(Q9))-((Fy6)*(L9)*@COS(Q9))+((m9)*g*(1-
0.513)*(L9)*@COS(Q9));

MO0 = m0*g*0.466*(L0)*@COS(Q0);

MOhr = MO1-((Fx1)*0.264*(Lf))-
((Fy1)*0.083*(Lf))+((mf)*g*0.315*(Lf));

MObr = MO1-((Fx1)*0.264*(Lf))+((Fy1)*0.662*(Lf))-
((mf)*g*0.43*(Lf));

MOhl = MO2-((Fx2)*0.264*(Lf))-
((Fy2)*0.083*(Lf))+((mf)*g*0.315*(Lf));

MObl = MO2-((Fx2)*0.264*(Lf))+((Fy2)*0.662*(Lf))-
((mf)*g*0.43*(Lf));

!ALLOWING IT TO TAKE ANY POSITIVE OR NEGATIVE VALUE;

@FREE(MO1);
@FREE(MO2);
@FREE(MO3);
@FREE(MO4);
@FREE(MO5);
@FREE(MO6);
@FREE(MO7);
```

```
@FREE(MO8);
@FREE(MO9);
@FREE(MO0);
@FREE(MOhr);
@FREE(MObr);
@FREE(MOhl);
@FREE(MObl);

!FORCE CALCULATIONS;

Fx1 = (1/2)*(Fxl+Fxr);
Fy1 = ((1/2)*(Fyl+Fyr-((m5+m6+m7+m8+m9+m0)*g)))-(m4*g)-(m1*g);

Fx2 = (1/2)*(Fxl+Fxr);
Fy2 = ((1/2)*(Fyl+Fyr-((m5+m6+m7+m8+m9+m0)*g)))-(m3*g)-(m2*g);

Fx3 = (1/2)*(Fxl+Fxr);
Fy3 = ((1/2)*(Fyl+Fyr-((m5+m6+m7+m8+m9+m0)*g)))-(m3*g);

Fx4 = (1/2)*(Fxl+Fxr);
Fy4 = ((1/2)*(Fyl+Fyr-((m5+m6+m7+m8+m9+m0)*g)))-(m4*g);

Fx5 = (Fxl+Fxr);
Fy5 = (Fyl+Fyr-((m5+m6+m7+m8+m9+m0)*g));

Fx6 = Fxr;
Fy6 = (Fyr-(m6*g));

Fx7 = Fxl;
Fy7 = (Fyl-(m7*g));

Fx8 = Fxl;
Fy8 = (Fyl-(m7*g)-(m8*g));

Fx9 = Fxr;
Fy9 = (Fyr-(m6*g)-(m9*g));

Fx0 = 0;
Fy0 = -m0*g;

!ALLOWING IT TO TAKE ANY POSITIVE OR NEGATIVE VALUE;

@FREE(Fx1);
@FREE(Fy1);
@FREE(Fx2);
@FREE(Fy2);
@FREE(Fx3);
@FREE(Fy3);
@FREE(Fx4);
@FREE(Fy4);
@FREE(Fx5);
@FREE(Fy5);
```

```
@FREE(Fx6);
@FREE(Fy6);
@FREE(Fx7);
@FREE(Fy7);
@FREE(Fx8);
@FREE(Fy8);
@FREE(Fx9);
@FREE(Fy9);
@FREE(Fx0);
@FREE(Fy0);

!ANTHROPOMETRY DATA;

!LINK LENGTHS;

L1 = 0.425646566;
L2 = 0.425646566;
L3 = 0.423916295;
L4 = 0.423916295;
L5 = 0.498317931;
L6 = 0.252619506;
L7 = 0.252619506;
L8 = 0.32183033;
L9 = 0.32183033;
L0 = 0.314909248;
Lf = 0.26300113;

!WEIGHTS;

m1 = 37.78811582/9.81;
m2 = 37.78811582/9.81;
m3 = 90.51571928/9.81;
m4 = 90.51571928/9.81;
m5 = 445.5482493/9.81;
m6 = 14.06069426/9.81;
m7 = 14.06069426/9.81;
m8 = 22.84862817/9.81;
m9 = 22.84862817/9.81;
m0 = 64.15191755/9.81;
mf = 13.18190087/9.81;

g = 9.81;

!CONSTRAINTS;

!CONSTRAINTS RELATED TO HANDS;

!LEFT HAND;

Yl=L1*@SIN(Q1)+L4*@SIN(Q4)+L5*@SIN(Q5)+L7*@SIN(Q7)+L8*@SIN(Q8)+(0.2
64*Lf);
```

```
!RIGHT HAND;

Yr=L1*@SIN(Q1)+L4*@SIN(Q4)+L5*@SIN(Q5)+L6*@SIN(Q6)+L9*@SIN(Q9)+(0.2
64*Lf);

!LINE OF SIGHT;

Xs = -(L6*@COS(Q6)+L9*@COS(Q9));
Ys = L1*@SIN(Q1)+L4*@SIN(Q4)+L5*@SIN(Q5)+(0.264*Lf);
Xn = -(L6*@COS(Q6)+L9*@COS(Q9)-L0*@COS(Q0p));
Yn = L1*@SIN(Q1)+L4*@SIN(Q4)+L5*@SIN(Q5)+L0*@SIN(Q0p)+(0.264*Lf);
X = (Xl+Xr)/2;
Y = (Yl+Yr)/2;
A = ((Xn-Xs)^2+(Yn-Ys)^2)^(1/2);
B = ((X-Xn)^2+(Y-Yn)^2)^(1/2);
C = ((X-Xs)^2+(Y-Ys)^2)^(1/2);
C^2 = A^2+B^2;

X > Xs;

Q0 >= Q0p-(10*Pi/180);

Q0 <= Q0p+(24*Pi/180);

!ALLOWING IT TO TAKE ANY POSITIVE OR NEGATIVE VALUE;

@FREE(Xs);
@FREE(Xn);
@FREE(X);

!CONSTRAINTS RELATED TO HUMAN BODY;

!RANGE OF MOTION (IN RADIANS);

Pi = 3.14159265359;

@BND(0.506145483078,Q3,4.71238898038);
@BND(0.506145483078,Q4,4.71238898038);
@BND(0.174532925199,Q5,2.35619449019);
@BND(-1.57079632679,Q6,1.57079632679);
@BND(-1.57079632679,Q7,1.57079632679);
@BND(-2.09439510239,Q8,1.74532925199);
@BND(-2.09439510239,Q9,1.74532925199);
@BND(0.34906585,Q0,2.09439510);

!LOWER BOUNDS;

Q1 >= 29*Pi/180;
Q2 >= 29*Pi/180;
Q3-Q2 >= 0*Pi/180;
Q4-Q1 >= 0*Pi/180;
Q5-Q4 >= -180*Pi/180;
```

```
Q5-Q3 >= -180*Pi/180;
Q6-Q9 >= 0*Pi/180;
Q7-Q8 >= 0*Pi/180;
Q8-Q5 >= -240*Pi/180;
Q9-Q5 >= -240*Pi/180;
Q0-Q5 >= -70*Pi/180;

!UPPER BOUNDS;

Q1 <= 153*Pi/180;
Q2 <= 153*Pi/180;
Q3-Q2 <= 174*Pi/180;
Q4-Q1 <= 174*Pi/180;
Q5-Q4 <= 50*Pi/180;
Q5-Q3 <= 50*Pi/180;
Q6-Q9 <= 180*Pi/180;
Q7-Q8 <= 180*Pi/180;
Q8-Q5 <= 10*Pi/180;
Q9-Q5 <= 10*Pi/180;
Q0-Q5 <= 30*Pi/180;

!ALLOWING IT TO TAKE ANY POSITIVE OR NEGATIVE VALUE;

@FREE(Q1);
@FREE(Q2);
@FREE(Q3);
@FREE(Q4);
@FREE(Q5);
@FREE(Q6);
@FREE(Q7);
@FREE(Q8);
@FREE(Q9);
@FREE(Q0);

!CONSTRAINTS RELATED TO THE FEET (BOTH FEET MUST BE ON FLOOR);

(L2*@SIN(Q2))+(L3*@SIN(Q3)) = (L1*@SIN(Q1))+(L4*@SIN(Q4));

!CONSTRAINTS RELATED TO THE SHOULDERS;

(L6*@COS(Q6))+(L9*@COS(Q9)) = (L7*@COS(Q7))+(L8*@COS(Q8))-Xl;

!CONSTRAINS RELATED TO BALANCE;

Xhr=-
((L6*@COS(Q6))+(L9*@COS(Q9))+(L5*@COS(Q5))+(L1*@COS(Q1))+(L4*@COS(Q
4))+(0.083*Lf));
Xhl=-
((L6*@COS(Q6))+(L9*@COS(Q9))+(L5*@COS(Q5))+(L2*@COS(Q2))+(L3*@COS(Q
3))+(0.083*Lf));
```

```
Xbr=-
((L6*@COS(Q6))+(L9*@COS(Q9))+(L5*@COS(Q5))+(L1*@COS(Q1))+(L4*@COS(Q
4))-(0.662*Lf));
Xbl=-
((L6*@COS(Q6))+(L9*@COS(Q9))+(L5*@COS(Q5))+(L2*@COS(Q2))+(L3*@COS(Q
3))-(0.662*Lf));

Xheel = @SMIN(Xhl, Xhr);
Xball = @SMAX(Xbl, Xbr);

X1=-(L6*@COS(Q6))-(L9*@COS(Q9))-(L5*@COS(Q5))-(L4*@COS(Q4))-
(0.371*L1*@COS(Q1));
X2=-(L6*@COS(Q6))-(L9*@COS(Q9))-(L5*@COS(Q5))-(L3*@COS(Q3))-
(0.371*L2*@COS(Q2));
X3=-(L6*@COS(Q6))-(L9*@COS(Q9))-(L5*@COS(Q5))-(0.372*L3*@COS(Q3));
X4=-(L6*@COS(Q6))-(L9*@COS(Q9))-(L5*@COS(Q5))-(0.372*L4*@COS(Q4));
X5=-(L6*@COS(Q6))-(L9*@COS(Q9))-0.62*(L5*@COS(Q5));
X6=(-0.61*(L6*@COS(Q6)));
X7=(-0.61*(L7*@COS(Q7)))+Xl;
X8=(-(L7*@COS(Q7)))-(0.513*L8*@COS(Q8))+Xl;
X9=(-(L6*@COS(Q6)))-(0.513*L9*@COS(Q9));
X0=(-(L6*@COS(Q6)))-(L9*@COS(Q9))+(0.466*L0*@COS(Q0));
Xfr=(-(L6*@COS(Q6)))-(L9*@COS(Q9))-(L5*@COS(Q5))-(L4*@COS(Q4))-
(L1*@COS(Q1))+((0.44-0.208)*Lf);
Xfl=(-(L6*@COS(Q6)))-(L9*@COS(Q9))-(L5*@COS(Q5))-(L3*@COS(Q3))-
(L2*@COS(Q2))+((0.44-0.208)*Lf);

!ALLOWING IT TO TAKE ANY POSITIVE OR NEGATIVE VALUE;

@FREE(Xhr);
@FREE(Xhl);
@FREE(Xbr);
@FREE(Xbl);
@FREE(Xfr);
@FREE(Xfl);
@FREE(Xheel);
@FREE(Xball);

!STABILITY CONSTRAINTS;

!PREVENT FROM TIPPING BACKWARD;

((Fxr*Yr)+(Fxl*Yl)-(Fyr*Xheel)-(Fyl*(Xl-Xheel))) <= 9.81*((m1*(X1-
Xheel))+(m2*(X2-Xheel))+(m3*(X3-Xheel))+(m4*(X4-Xheel))+(m5*(X5-
Xheel))+(m6*(X6-Xheel))+(m7*(X7-Xheel))+(m8*(X8-Xheel))+(m9*(X9-
Xheel))+(m0*(X0-Xheel))+(mf*(Xfr-Xheel))+(mf*(Xfl-Xheel)));

!PREVENT FROM TIPPING FORWARD;

((Fxr*Yr)+(Fxl*Yl)-(Fyr*Xball)-(Fyl*(Xl-Xball))) >= 9.81*((m1*(x1-
Xball))+(m2*(X2-Xball))+(m3*(X3-Xball))+(m4*(X4-Xball))+ (m5*(X5-
```

```
Xball))+(m6*(X6-Xball))+(m7*(X7-Xball))+(m8*(X8-Xball))+(m9*(X9-
Xball))+(m0*(X0-Xball))+(mf*(Xfr-Xball))+(mf*(Xfl-Xball)));

!ALLOWING IT TO TAKE ANY POSITIVE OR NEGATIVE VALUE;

@FREE(X1);
@FREE(X2);
@FREE(X3);
@FREE(X4);
@FREE(X5);
@FREE(X6);
@FREE(X7);
@FREE(X8);
@FREE(X9);
@FREE(X0);

!CONVERTS RADIANS TO DEGREES;

D1 = Q1*180/Pi;
D2 = Q2*180/Pi;
D3 = Q3*180/Pi;
D4 = Q4*180/Pi;
D5 = Q5*180/Pi;
D6 = Q6*180/Pi;
D7 = Q7*180/Pi;
D8 = Q8*180/Pi;
D9 = Q9*180/Pi;
D0 = Q0*180/Pi;
D0p = Q0p*180/Pi;

!ALLOWING IT TO TAKE ANY POSITIVE OR NEGATIVE VALUE;

@FREE(D1);
@FREE(D2);
@FREE(D3);
@FREE(D4);
@FREE(D5);
@FREE(D6);
@FREE(D7);
@FREE(D8);
@FREE(D9);
@FREE(D0);
@FREE(D0p);

!INITIAL SOLUTION;

INIT:
!(IN DEGREES);
D1 = 75;
D2 = 75;
D3 = 170;
D4 = 170;
```

```
D5 = 45;
D6 = -25;
D7 = -25;
D8 = -90;
D9 = -90;
D0 = 45;

ENDINIT

!EXPORT RESULTS TO THE EXCEL FILE;

DATA:

@OLE( 'C:\My Documents\posture--righthand.XLS','DEG1')= D1;
@OLE( 'C:\My Documents\posture--righthand.XLS','DEG2')= D2;
@OLE( 'C:\My Documents\posture--righthand.XLS','DEG3')= D3;
@OLE( 'C:\My Documents\posture--righthand.XLS','DEG4')= D4;
@OLE( 'C:\My Documents\posture--righthand.XLS','DEG5')= D5;
@OLE( 'C:\My Documents\posture--righthand.XLS','DEG6')= D6;
@OLE( 'C:\My Documents\posture--righthand.XLS','DEG7')= D7;
@OLE( 'C:\My Documents\posture--righthand.XLS','DEG8')= D8;
@OLE( 'C:\My Documents\posture--righthand.XLS','DEG9')= D9;
@OLE( 'C:\My Documents\posture--righthand.XLS','DEG0')= D0;

ENDDATA

!END EXPORT RESULTS TO THE EXCEL FILE;

END

!THE END OF THE PROGRAM;
```

APPENDIX D: Examples of Results from Posture Prediction Model

Hand Load (N)

	Left	Right
Fx	50	50
Fy	0	0

Hand Position

	Left	Right
X Position (meters)	0	0
Y Position (meters)	1.5	1.5

Posture

	Left	Right
Neck (deg. From hor.)	77.6002	
Elbow (deg. From hor.)	30.84332	30.84332
Shoulder (deg. From hor.)	30.84332	30.84332
Hip (deg. From hor.)	63.83869	
Knee (deg. From hor.)	100.8021	125.9314
Ankle (deg. From hor.)	39.78568	125.7302

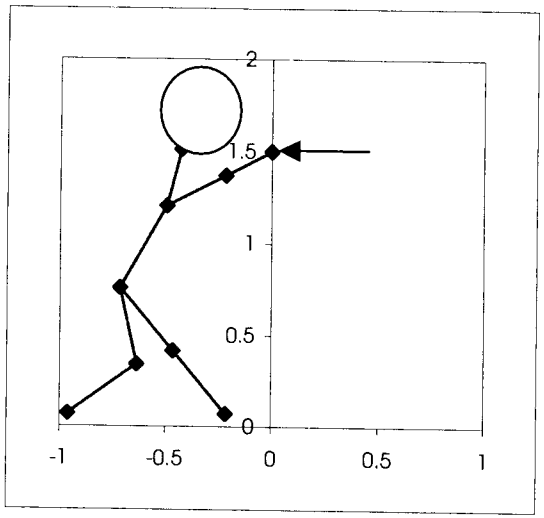

Hand Load (N)

	Left	Right
Fx	35.35	35.35
Fy	35.35	35.35

Hand Position

	Left	Right
X Position (meters)	0	0
Y Position (meters)	1.5	1.5

Posture

	Left	Right
Neck (deg. From hor.)	88.12498	
Elbow (deg. From hor.)	90	90
Shoulder (deg. From hor.)	19.74543	19.74543
Hip (deg. From hor.)	62.09041	
Knee (deg. From hor.)	116.3085	132.7013
Ankle (deg. From hor.)	35.77857	131.7963

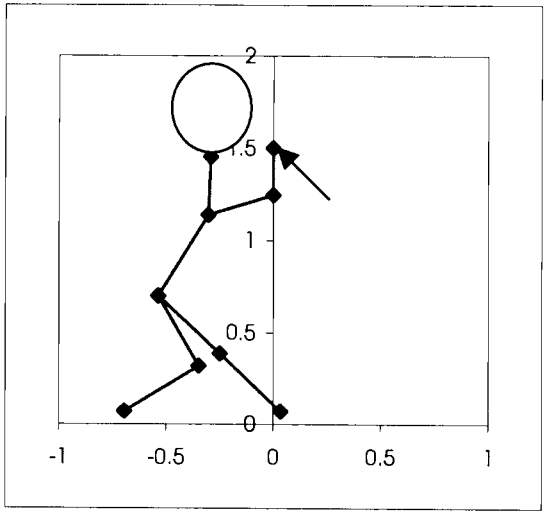

Hand Load (N)

	Left	Right
Fx	0	0
Fy	50	50

Hand Position

	Left	Right
X Position (meters)	0	0
Y Position (meters)	1.5	1.5

Posture

	Left	Right
Neck (deg. From hor.)	98.59948	
Elbow (deg. From hor.)	90	90
Shoulder (deg. From hor.)	32.16429	32.16429
Hip (deg. From hor.)	68.59948	
Knee (deg. From hor.)	133.7847	141.5708
Ankle (deg. From hor.)	33.77291	139.0127

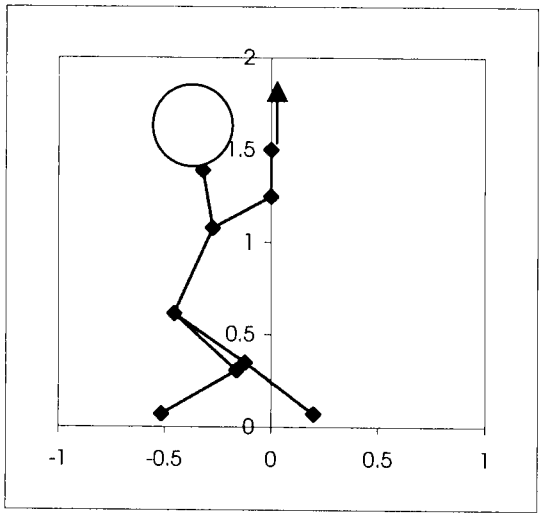

Hand Load (N)

	Left	Right
Fx	-35.35	-35.35
Fy	35.35	35.35

Hand Position

	Left	Right
X Position (meters)	0	0
Y Position (meters)	1.5	1.5

Posture

	Left	Right
Neck (deg. From hor.)	115.1541	
Elbow (deg. From hor.)	60.99486	60.99486
Shoulder (deg. From hor.)	60.99486	60.99486
Hip (deg. From hor.)	112.0912	
Knee (deg. From hor.)	147.7473	148.6437
Ankle (deg. From hor.)	34.35629	144.7196

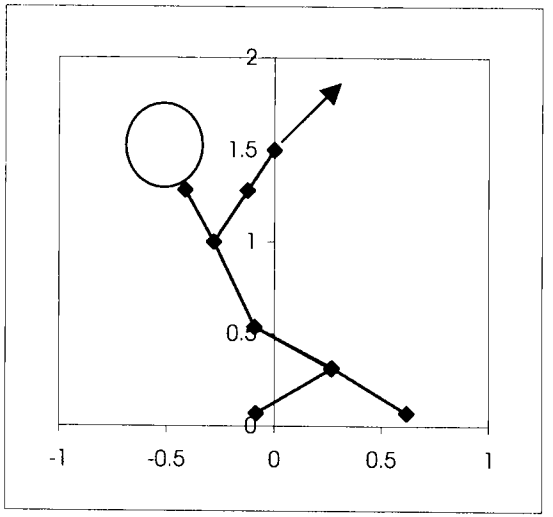

Hand Load (N)

	Left	Right
Fx	-50	-50
Fy	0	0

Hand Position

	Left	Right
X Position (meters)	0	0
Y Position (meters)	1.5	1.5

Posture

	Left	Right
Neck (deg. From hor.)	120	
Elbow (deg. From hor.)	43.57744	43.57744
Shoulder (deg. From hor.)	43.57744	43.57744
Hip (deg. From hor.)	130.9554	
Knee (deg. From hor.)	129.2132	144.0916
Ankle (deg. From hor.)	129.2132	74.22572

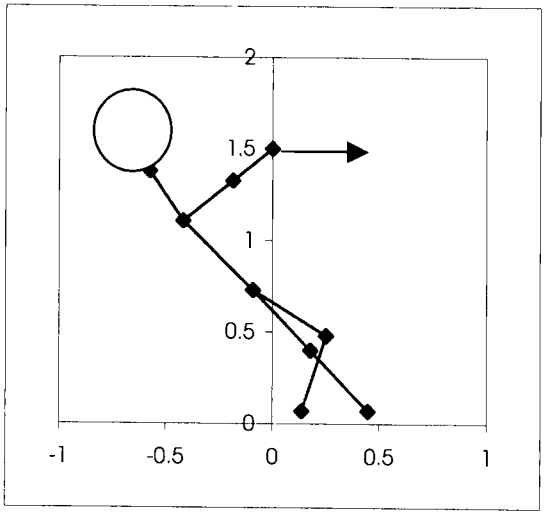

Hand Load (N)

	Left	Right
Fx	-35.35	-35.35
Fy	-35.35	-35.35

Hand Position

	Left	Right
X Position (meters)	0	0
Y Position (meters)	1.5	1.5

Posture

	Left	Right
Neck (deg. From hor.)	71.72789	
Elbow (deg. From hor.)	90	90
Shoulder (deg. From hor.)	3.365158	3.365158
Hip (deg. From hor.)	117.4954	
Knee (deg. From hor.)	122.4358	131.7586
Ankle (deg. From hor.)	122.4358	70.32716

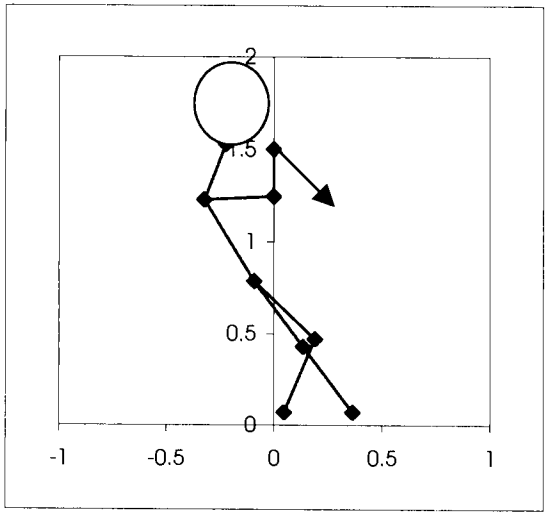

Hand Load (N)

	Left	Right
Fx	0	0
Fy	-50	-50

Hand Position

	Left	Right
X Position (meters)	0	0
Y Position (meters)	1.5	1.5

Posture

	Left	Right
Neck (deg. From hor.)	56.64795	
Elbow (deg. From hor.)	90	90
Shoulder (deg. From hor.)	-8.409761	-8.409761
Hip (deg. From hor.)	107.1508	
Knee (deg. From hor.)	118.1807	120.9801
Ankle (deg. From hor.)	118.1807	64.88807

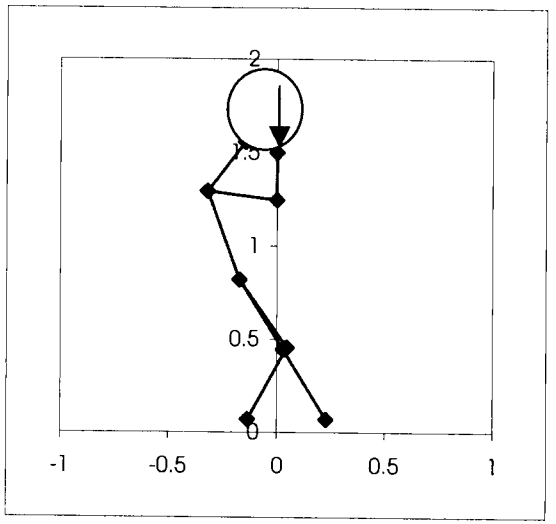

Hand Load (N)

	Left	Right
Fx	35.35	35.35
Fy	-35.35	-35.35

Hand Position

	Left	Right
X Position (meters)	0	0
Y Position (meters)	1.5	1.5

Posture

	Left	Right
Neck (deg. From hor.)	24	
Elbow (deg. From hor.)	90	90
Shoulder (deg. From hor.)	-11.90398	-11.90398
Hip (deg. From hor.)	94	
Knee (deg. From hor.)	114.7533	119.4552
Ankle (deg. From hor.)	58.33013	117.3379

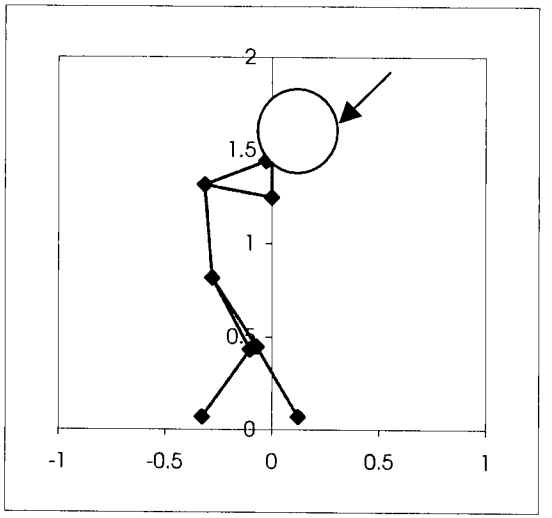

Hand Load (N)

	Left	Right
Fx	50	50
Fy	0	0

Hand Position

	Left	Right
X Position (meters)	0	0
Y Position (meters)	1	1

Posture

	Left	Right
Neck (deg. From hor.)	24	
Elbow (deg. From hor.)	17.36865	17.36865
Shoulder (deg. From hor.)	-76.74184	-76.74184
Hip (deg. From hor.)	84.86173	
Knee (deg. From hor.)	103.636	128.3584
Ankle (deg. From hor.)	37.67132	127.0569

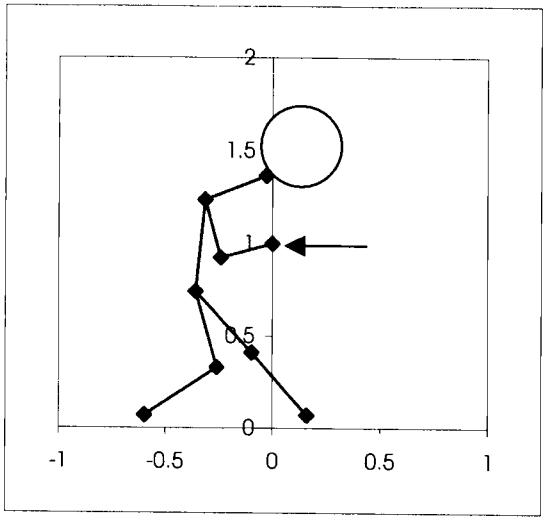

Hand Load (N)

	Left	Right
Fx	35.35	35.35
Fy	35.35	35.35

Hand Position

	Left	Right
X Position (meters)	0	0
Y Position (meters)	1	1

Posture

	Left	Right
Neck (deg. From hor.)	63.36584	
Elbow (deg. From hor.)	-17.39104	-17.39104
Shoulder (deg. From hor.)	-17.39104	-17.39104
Hip (deg. From hor.)	73.48721	
Knee (deg. From hor.)	117.0557	133.3362
Ankle (deg. From hor.)	35.46715	132.0297

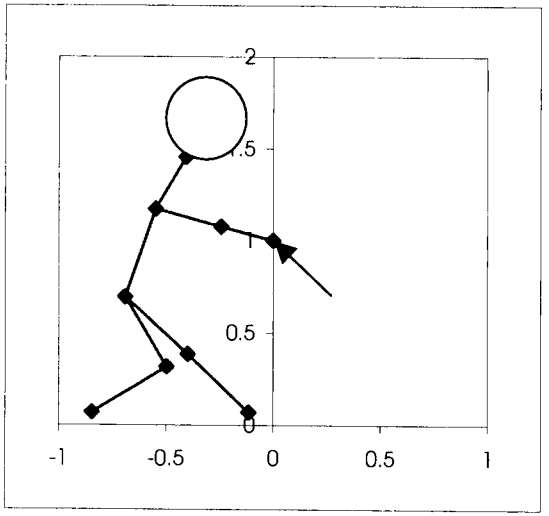

Hand Load (N)

	Left	Right
Fx	0	0
Fy	50	50

Hand Position

	Left	Right
X Position (meters)	0	0
Y Position (meters)	1	1

Posture

	Left	Right
Neck (deg. From hor.)	88.18556	
Elbow (deg. From hor.)	90	90
Shoulder (deg. From hor.)	19.8129	19.8129
Hip (deg. From hor.)	58.18556	
Knee (deg. From hor.)	207.1621	188.2658
Ankle (deg. From hor.)	52.77655	29

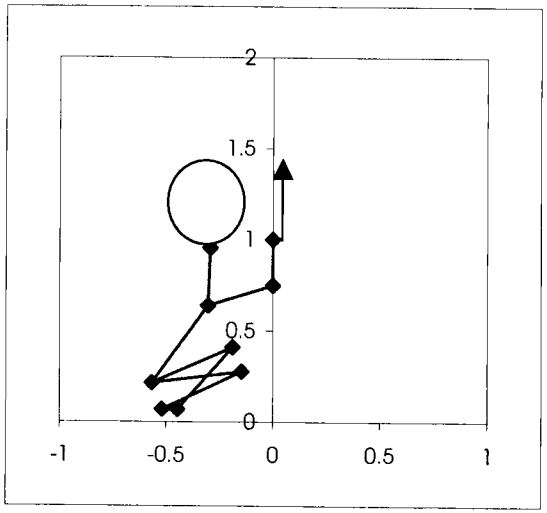

Hand Load (N)

	Left	Right
Fx	-35.35	-35.35
Fy	35.35	35.35

Hand Position

	Left	Right
X Position (meters)	0	0
Y Position (meters)	1	1

Posture

	Left	Right
Neck (deg. From hor.)	89.773	
Elbow (deg. From hor.)	43.01611	43.01611
Shoulder (deg. From hor.)	43.01611	43.01611
Hip (deg. From hor.)	87.8145	
Knee (deg. From hor.)	243.2841	203
Ankle (deg. From hor.)	80.15788	29

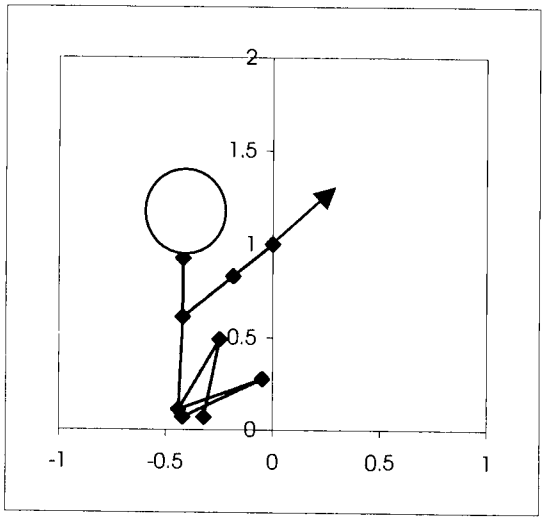

Hand Load (N)

	Left	Right
Fx	-50	-50
Fy	0	0

Hand Position

	Left	Right
X Position (meters)	0	0
Y Position (meters)	1	1

Posture

	Left	Right
Neck (deg. From hor.)	58.80819	
Elbow (deg. From hor.)	-9.544264	-9.544264
Shoulder (deg. From hor.)	-30.53283	-30.53283
Hip (deg. From hor.)	108.4164	
Knee (deg. From hor.)	128.6857	143.0883
Ankle (deg. From hor.)	128.6857	73.71091

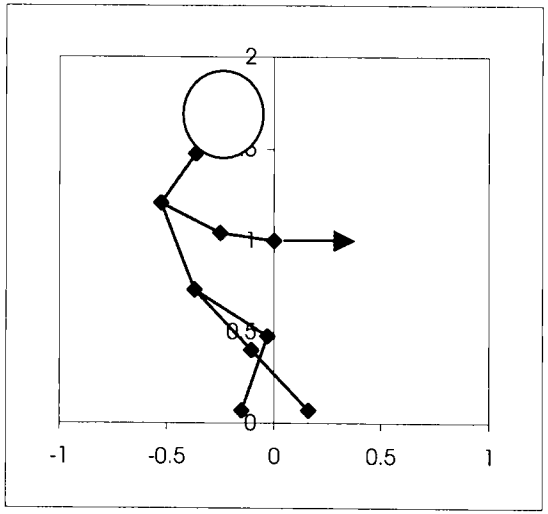

Hand Load (N)

	Left	Right
Fx	-35.35	-35.35
Fy	-35.35	-35.35

Hand Position

	Left	Right
X Position (meters)	0	0
Y Position (meters)	1	1

Posture

	Left	Right
Neck (deg. From hor.)	38.80452	
Elbow (deg. From hor.)	82.88018	82.88018
Shoulder (deg. From hor.)	-31.92763	-31.92763
Hip (deg. From hor.)	108.8045	
Knee (deg. From hor.)	182.2457	156.0598
Ankle (deg. From hor.)	68.12037	29

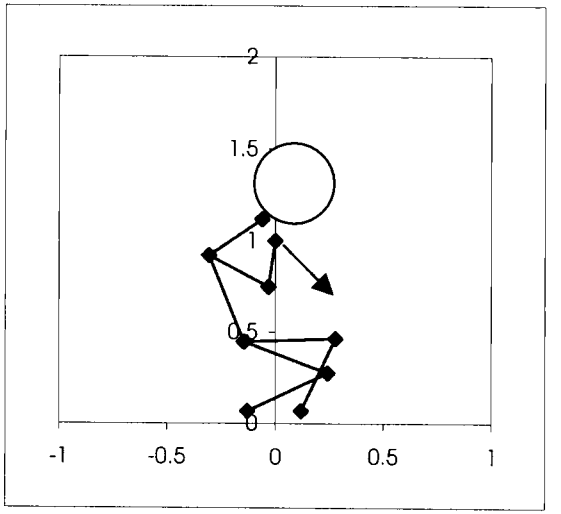

Hand Load (N)

	Left	Right
Fx	0	0
Fy	-50	-50

Hand Position

	Left	Right
X Position (meters)	0	0
Y Position (meters)	1	1

Posture

	Left	Right
Neck (deg. From hor.)	37.34028	
Elbow (deg. From hor.)	-41.96782	-41.96782
Shoulder (deg. From hor.)	-44.53716	-44.53716
Hip (deg. From hor.)	107.3403	
Knee (deg. From hor.)	89.68762	90.31238
Ankle (deg. From hor.)	89.68762	90.31238

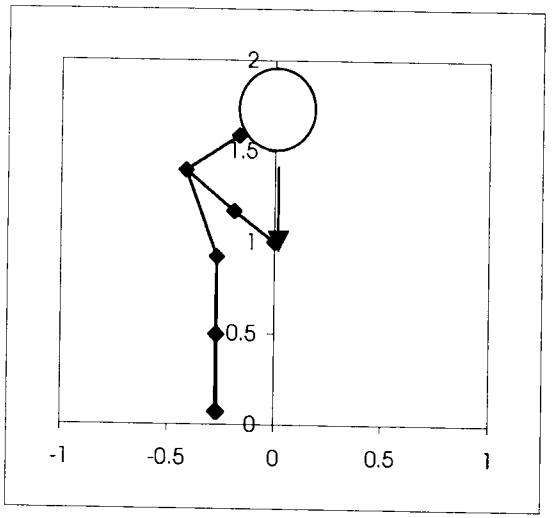

Hand Load (N)

	Left	Right
Fx	35.35	35.35
Fy	-35.35	-35.35

Hand Position

	Left	Right
X Position (meters)	0	0
Y Position (meters)	1	1

Posture

	Left	Right
Neck (deg. From hor.)	44.30566	
Elbow (deg. From hor.)	-2.5777652	-2.5777652
Shoulder (deg. From hor.)	-2.627476	-2.627476
Hip (deg. From hor.)	14.30566	
Knee (deg. From hor.)	101.1501	101.1417
Ankle (deg. From hor.)	101.1334	101.1417

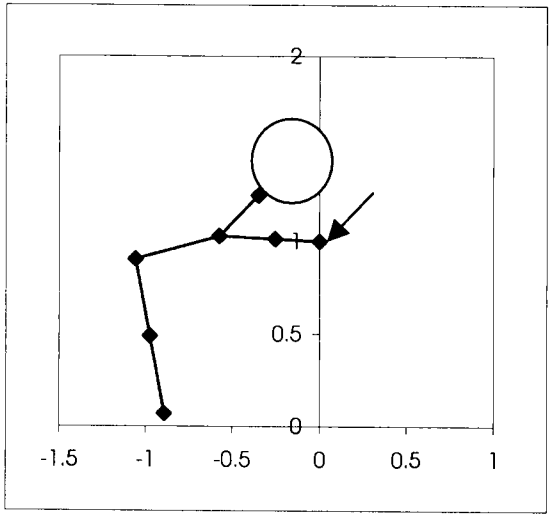

Hand Load (N)

	Left	Right
Fx	50	50
Fy	0	0

Hand Position

	Left	Right
X Position (meters)	0	0
Y Position (meters)	0.5	0.5

Posture

	Left	Right
Neck (deg. From hor.)	44.65355	
Elbow (deg. From hor.)	1.065724	1.065724
Shoulder (deg. From hor.)	-4.512048	-4.512048
Hip (deg. From hor.)	59.43553	
Knee (deg. From hor.)	239.4355	239.4355
Ankle (deg. From hor.)	65.43553	65.43553

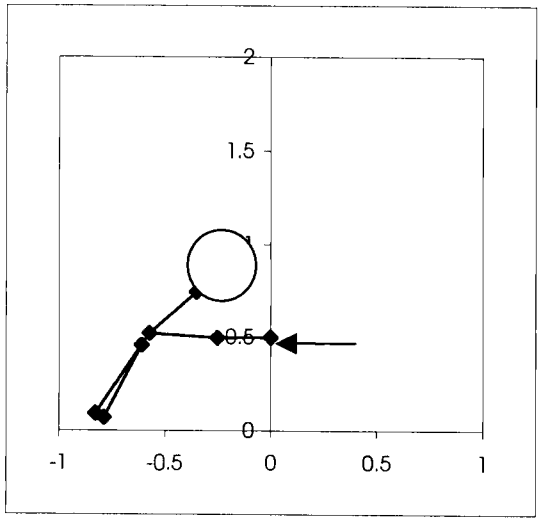

Hand Load (N)

	Left	Right
Fx	35.35	35.35
Fy	35.35	35.35

Hand Position

	Left	Right
X Position (meters)	0	0
Y Position (meters)	0.5	0.5

Posture

	Left	Right
Neck (deg. From hor.)	27.84555	
Elbow (deg. From hor.)	-52.844	-52.91133
Shoulder (deg. From hor.)	-52.96415	-52.91133
Hip (deg. From hor.)	54.99009	
Knee (deg. From hor.)	139.6792	139.6792
Ankle (deg. From hor.)	29	29

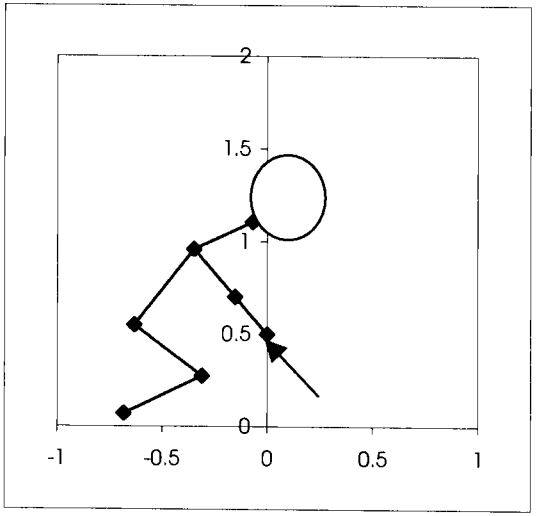

Hand Load (N)

	Left	Right
Fx	0	0
Fy	50	50

Hand Position

	Left	Right
X Position (meters)	0	0
Y Position (meters)	0.5	0.5

Posture

	Left	Right
Neck (deg. From hor.)	24	
Elbow (deg. From hor.)	-56.75688	-56.75688
Shoulder (deg. From hor.)	-56.75688	-56.75688
Hip (deg. From hor.)	53.84351	
Knee (deg. From hor.)	140.0433	146.7252
Ankle (deg. From hor.)	33.74103	139.5629

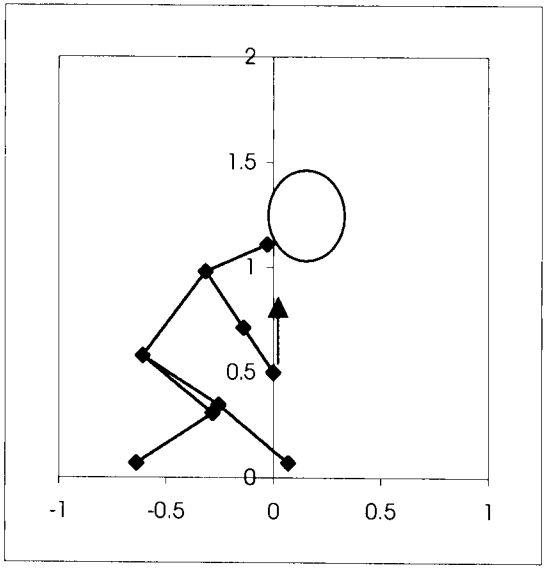

Hand Load (N)

	Left	Right
Fx	-35.35	-35.35
Fy	35.35	35.35

Hand Position

	Left	Right
X Position (meters)	0	0
Y Position (meters)	0.5	0.5

Posture

	Left	Right
Neck (deg. From hor.)	24	
Elbow (deg. From hor.)	-56.75688	-56.75688
Shoulder (deg. From hor.)	-56.75688	-56.75688
Hip (deg. From hor.)	78.73918	
Knee (deg. From hor.)	149.3785	152.9647
Ankle (deg. From hor.)	29	147.3564

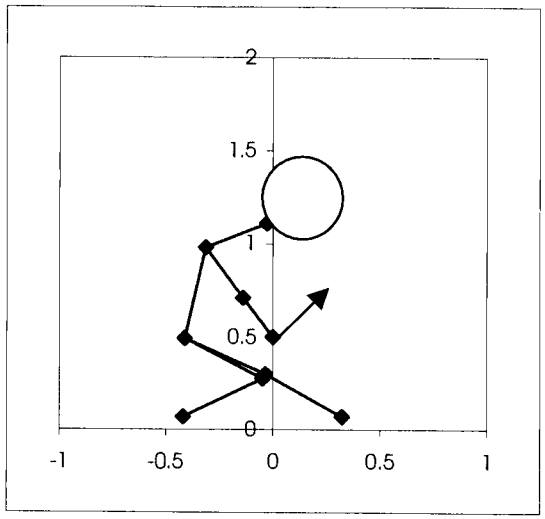

Hand Load (N)

	Left	Right
Fx	-50	-50
Fy	0	0

Hand Position

	Left	Right
X Position (meters)	0	0
Y Position (meters)	0.5	0.5

Posture

	Left	Right
Neck (deg. From hor.)	31.40989	
Elbow (deg. From hor.)	-41.69924	-41.69924
Shoulder (deg. From hor.)	-54.90236	-54.90236
Hip (deg. From hor.)	93.44995	
Knee (deg. From hor.)	158.0941	157.249
Ankle (deg. From hor.)	29	151.8864

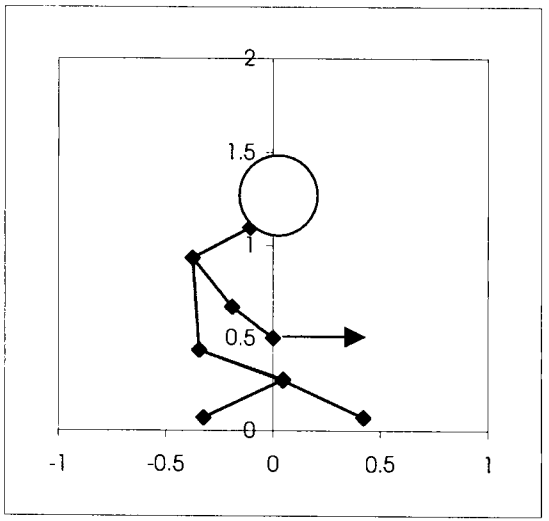

Hand Load (N)

	Left	Right
Fx	-35.35	-35.35
Fy	-35.35	-35.35

Hand Position

	Left	Right
X Position (meters)	0	0
Y Position (meters)	0.5	0.5

Posture

	Left	Right
Neck (deg. From hor.)	74.59305	
Elbow (deg. From hor.)	-6.16383	-6.16383
Shoulder (deg. From hor.)	-6.16383	-6.16383
Hip (deg. From hor.)	98.49649	
Knee (deg. From hor.)	270	270
Ankle (deg. From hor.)	96	96

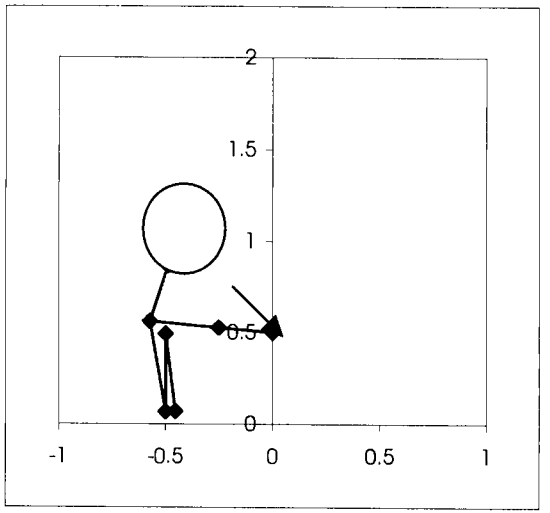

Hand Load (N)

	Left	Right
Fx	0	0
Fy	-50	-50

Hand Position

	Left	Right
X Position (meters)	0	0
Y Position (meters)	0.5	0.5

Posture

	Left	Right
Neck (deg. From hor.)	70.2367	
Elbow (deg. From hor.)	-10.52018	-10.52018
Shoulder (deg. From hor.)	-10.52018	-10.52018
Hip (deg. From hor.)	96.87821	
Knee (deg. From hor.)	241.9495	203
Ankle (deg. From hor.)	77.06203	29

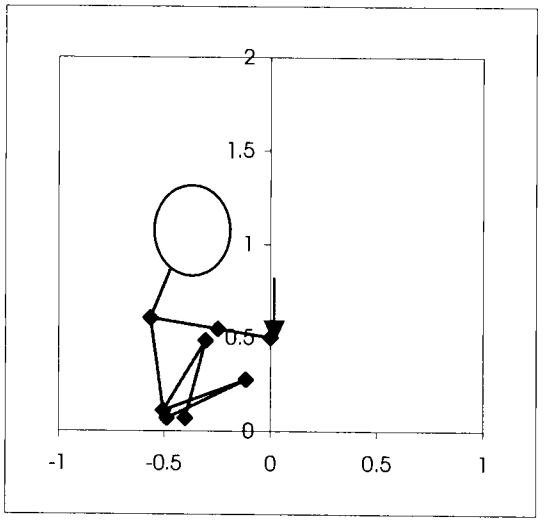

Hand Load (N)

	Left	Right
Fx	35.35	35.35
Fy	-35.35	-35.35

Hand Position

	Left	Right
X Position (meters)	0	0
Y Position (meters)	0.5	0.5

Posture

	Left	Right
Neck (deg. From hor.)	24	
Elbow (deg. From hor.)	50.86873	50.86873
Shoulder (deg. From hor.)	-61.11091	-61.11091
Hip (deg. From hor.)	72.65991	
Knee (deg. From hor.)	240.6113	203
Ankle (deg. From hor.)	74.45823	29